Effect of concrete cover on the pure torsional behavior of reinforced concrete beams
Analytical model

Ibrahim, Mohammed Sirage; Gebreyouhannes, Esayas

DOI
10.1016/j.engstruct.2024.118912

Publication date
2024

Document Version
Final published version

Published in
Engineering Structures

Engineering Structures 321 (2024) 118912

Contents lists available at ScienceDirect

Engineering Structures

journal homepage: www.elsevier.com/locate/engstruct

Effect of concrete cover on the pure torsional behavior of reinforced concrete beams: Analytical model

Mohammed Sirage Ibrahim [a,b], Esayas Gebreyouhannes [b,*]

[a] Delft University of Technology, Faculty of Civil Engineering and Geosciences, Stevinweg 1, 2628 CN, Delft, the Netherland
[b] Addis Ababa University, School of Civil and Environmental Engineeering, King George VI Street, Addis Ababa, 385, Ethiopia

ARTICLE INFO

Keywords:
Torsion
Concrete cover spalling
CFT
STM
SMMT

ABSTRACT

Experimental data on RC members subjected to pure torsion is compiled from published studies so far. Interestingly, the past studies have concentrated largely on members with small to moderate concrete covers, with handful data on members with thick concrete cover. Widely accepted torsion models including the diagonal compression field theory (CFT), softened truss model (STM) and softened membrane model for torsion (SMMT) are verified on the domains of experimental data missing-in specimens with thick concrete cover. With increasing demand for durability design of RC structures use of thick concrete cover, say up to 75 mm, is being introduced in practice. Recent experimental investigation by the authors demonstrated that spalling of concrete cover, particularly in cases of thick covers, significantly impacts the torsional behavior of RC members. The present study uses these set of experiments to look at the response prediction capability of the existing advanced models and assess the reliability of existing concrete cover spalling theories. For cases with thick cover, the existing models either did not adequately capture the ultimate capacity or erroneously predicted the torsional behavior of the members due to the different mechanics between RC beams with thin and thick covers. Similarly, the spalling theories failed to fully explain the physically observed spalling behavior. Guided by the recent experimental observations and the apparent gaps, the study provides a rational theory for the spalling of concrete cover. The initiation and gradual evolution of concrete cover spalling is traced by observing the acting spalling moment and spalling resistance formulated in the proposed spalling model. The proposed spalling model inherently assumes members susceptibility to spalling of cover concrete and is governed by, the thickness of the concrete cover, tensile strength of concrete, presence of rebar cage and their location, and size of the member. The theory is unified and can explain the spalling of cover due to torsion as well as shear. Its capability is examined by integrating the approach into existing truss model. When compared with state-of-the-art models, the proposed method provides consistent prediction with a relatively smaller scatter, for cases with thick concrete cover as well.

1. Introduction

The torsional behavior of reinforced concrete (RC) members depends on different factors. The main variables include the amount of reinforcement, concrete strength, the shape of the member, width to depth ratio, and concrete cover [1–6]. Over the last fifty years, a surge of research has been observed focusing on the mechanistic behavior of RC members subjected to pure torsion [7]. Noteworthy, previous studies have mainly focused on certain areas of investigations while other variables are least explored. To examine the accumulated experimental data distribution and explore remaining research gaps, a pure torsional experiment database is carefully compiled from published studies. Fig. 1 shows pure torsional experiments [1–4,7–15] presented in terms of compressive strength of the concrete and reinforcement ratio. The plot is prepared using experimental data of more than 175 solid rectangular RC specimens. It is evident that concrete strength from normal to high strength and rebar ratios from under to over reinforced cases are satisfactorily covered.

While it is reasonable for the studies to be concentrated on normal strength concrete and under-reinforced regions, the database also points to regions in which further studies may be needed. Fig. 2 shows the distribution of pure torsion experimental studies regarding concrete cover thickness. The vertical axis describes the relationship between the

* Correspondence to: Addis Ababa University, School of Civil and Environmental Engineering, Addis Ababa, Ethiopia.
E-mail addresses: M.S.Ibarhim-1@tudelft.nl (M.S. Ibrahim), esayas.gebreyohannes@aait.edu.et, gyisu@yahoo.com (E. Gebreyouhannes).

https://doi.org/10.1016/j.engstruct.2024.118912
Received 17 April 2024; Received in revised form 20 August 2024; Accepted 30 August 2024
Available online 9 September 2024

Nomenclature

A_c	Area enclosed within the outer perimeter of the cross-section.
A_l	Total area of longitudinal reinforcement.
$A_{l,i}$	Local area of longitudinal reinforcement on panel i.
A_t	Area of a single leg of transverse reinforcement.
b	Width of a member (Figure1 and Figure2).
C_C	Clear cover.
f_c	Compressive strength of concrete.
f_{ct}	Tensile strength of concrete.
f_{ul}	Ultimate strength of longitudinal reinforcement.
f_{ut}	Ultimate strength of transverse reinforcement.
f_{yl}	Yield strength of longitudinal reinforcement.
f_{yt}	Yield strength of transverse reinforcement.
q_c	In-plane shear flow.
S	Spacing of transverse reinforcement.
T	Torsion.
T_c	Acting spalling torsion.
T_{cr}	Cracking torsion.
t_d	Thickness of shear flow zone.
T_{spall}	Spalling resistance.
T_{ult}	Ultimate torsional capacity of tested specimen.
ε_1	Smeared biaxial strain in the 1-direction (SMMT model).
ε_2	Smeared biaxial strain in the 2-direction (SMMT model).
$\varepsilon_{\lim it}$	Maximum strain in the 2-direction.
γ_{12}	Average shear strain in the 2–1 coordinate (SMMT model).
ϕ_l	Diameter of longitudinal rebar.
ϕ_t	Diameter of transverse rebar.
θ	Angle of inclination from the horizontal axis (Eq. 4).
θ	Angle of twist.
τ	Shear stress due to torsion.

concrete cover and the full sectional property. Rahal and Collins [6,30] used this criterion to show the susceptibility to cover spalling. The plot clearly shows the lack of studies on thick concrete cover. Nearly all the torsional tests are conducted for members with a small concrete cover. The average normalized concrete cover ratio of the specimens is 0.29. For such members, concrete strength and the relative amount of longitudinal and transverse reinforcement play a major role in the failure mechanism. Failure is usually associated with the crushing of softened diagonal strut or rebar rupture. On the contrary, for sections with thick concrete cover, the torsional behavior is controlled by premature cover spalling phenomena (see Fig. 3). Yet, studies pertaining to this brittle type of failure is almost non-existent.

In practice, due to the increasing demand for durability design, recent code provisions propose thick concrete covers considering the environmental exposure of the structural member. ACI [16] allows the use of up to 75 mm cover for members in an aggressive environment. Similarly, according to EC 2 [17] structural members with high exposure class requirements might be designed with a specified cover of more than 70 mm, considering the cover needed for deviation during construction. Accordingly, the maximum normalized cover ratio for each specimen is calculated assuming a cover limit of 75 mm, and the average value is 1.03 as indicated in Fig. 2. The absence of investigation on the thick concrete cover is plainly depicted from the gap between the average (0.29) and the allowable limit (1.03).

Despite its brittle failure, provision for torsion didn't appear in the codes until 1971 when the first time a design guideline was given in ACI [31]. Beginning the 1950s torsional theories followed two distinct paths in skew bending theory and formulations-based membrane element truss model. The skew bending theory includes the works by Lessig [18], Yudin [19], Collins et.al. [20], Hsu [21], and Elfgren [22,23]. The research path using the truss model include the theories of Lampert and Thürlimann [24], Collins [25], Mitchell and Collins [5], Collins and Mitchell [26], Hsu and Mo [27], and Jeng and Hsu [28]. The skew bending theory only used equilibrium equations and can only predict the ultimate capacity of members. In contrast, the modern truss model-based theories incorporate the three Navier's principles of mechanics. The advanced truss models such as the diagonal compression field theory(CFT) [5], softened truss model(STM) [27], and softened membrane model for torsion(SMMT) [28] can predict the entire load history.

In the truss model, in view of the direction, gradual formation, rotation of cracks and crack modeling, two types of smeared truss model theories have been developed, namely, the rotating angle theory [5,29, 32] and the fixed angle theory [28,33].

Mitchell and Collins [5] proposed a diagonal compression field theory (CFT) with a rotating angle truss model satisfying the three principles of mechanics. The model is one of the first rational approaches that can predict the torsional behavior of RC members. The model assumes concrete will not carry any tension after cracking and the shear flow due to torsion is assumed to be resisted by a diagonal compression field. Using equilibrium, compatibility equations, and material constitutive law for concrete in compression, CFT can trace the full history of RC members subjected to torsion. In CFT not all of the concrete is effective in providing diagonal compressive stresses. Mitchell and Collins observed the spalling of concrete cover and assumed the spall off concrete at corners results in a reduction to the effective thickness of shear flow. Accordingly, CFT models the behavior of RC beams subjected to torsion using this net effective thickness and uniaxial compression strength of concrete without compression softening effect.

In 1985 Hsu and Mo proposed a rotating angle softened truss model (STM). STM [27] is constructed on satisfying Navier's principle of mechanics of material. The model implemented a similar equilibrium and compatibility model to that of the CFT. Unlike CFT, STM utilizes softened constitutive model for cracked concrete in compression and incorporates a smeared tensile stress-strain relationship for rebar. Extending the softened membrane model (SMM) for shear by Hsu and Zhu [34], Jeng and Hsu proposed a softened membrane model for torsion (SMMT). SMMT is a fixed angle smeared truss model and in addition to Navier's principle of mechanics, it incorporated the Poisson effect for concrete subjected to biaxial stress condition. SMMT model can predict the entire load history curve, including the ranges before and after cracking, as well as the ascending and descending branches.

The above theoretical models inherently assume the ultimate capacity of the members to be controlled by either crushing of the softened concrete or rebar rupture. While they acknowledge concrete cover spalling may control the behavior of members, in both STM and SMMT the effect of concrete cover is not considered in their formulation. CFT considers the spalling of cover by using the spalled concrete section for analysis. While it rightly considers spalling, the model uses a uniaxial stress-strain model for concrete in compression and ignore the contribution of cracked concrete in tension. Although at the time it was not quantified, the use of uniaxial stress-strain models seems incompatible as it is proven compression softening occurs due to transverse cracking on their landmark theory MCFT by Vecchio and Collins [29]. In addition, the spalling of cover does not initiate from the start. Although, it may serve as a simplistic/ conservative design assumption, considering spalled section throughout the whole range cannot be physically explained.

To better understand the effect of the concrete cover and to illustrate the difference between the theoretical models, their prediction is examined with the experimental results of Nagataki et al. [14] (See Fig. 2 for the experiments and Fig. 4 for the comparison). For specimens with small cover C1, the behavior of the member is adequately predicted by the models. However, for the specimens with large cover, the prediction by the models differs by large. SMMT's prediction is consistent with the experimental results in the pre-cracking range, while it highly overestimates the ultimate capacity and erroneously predicted the failure mode. The ultimate capacity predicted by CFT is on the safe side with a sufficiently close estimate. However, the behavior of the thick cover specimens is not adequately captured as the model projected the member to reach peak capacity after a large angle of twist, which is contrary to the observed behavior. It should also be noticed that the difference between the experiment and the models predictions increases with the increase of the concrete cover thickness.

On the other hand, due to stringent requirement for durability design in code provisions, currently, structures may be designed with a relatively larger concrete cover. The torsional behavior of such structural elements cannot be adequately captured using the exiting advanced models. Therefore, it is useful to close this gap.

While spalling of concrete cover may lead to brittle failure in torsion and shear loaded members, the mechanics of spalling of concrete cover is not adequately investigated and remains still a mystery. Mitchell and Collins [5] for pure torsional members and Rahal and Collins [6,30] for members subjected to combined torsion and shear investigated and proposed the mechanics of spalling of cover concrete. Without a doubt, the investigations on the concrete cover [5,6,30] provide a useful insight into the torsional behavior of RC members. However, the proposed spalling mechanism cannot explain the initiation and gradual evolution of concrete cover spalling. The theory also lacks generality as it cannot explain spalling in shell elements. Furthermore, in some cases, the

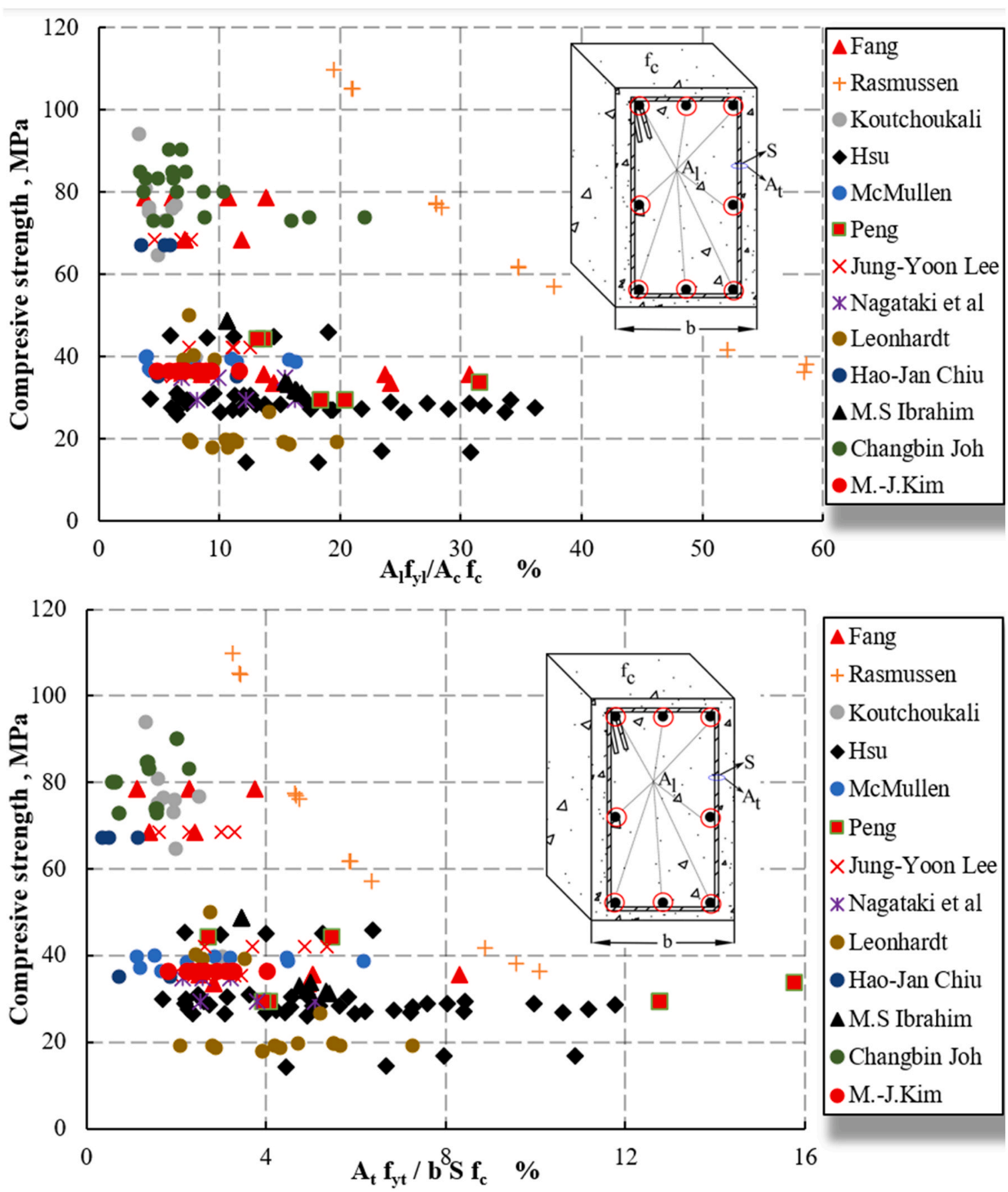

Fig. 1. -Experimental researches pertaining to the compressive strength of concrete against reinforcement ratio.

assumptions seem to be incompatible with experimentally observed behavior (see Section 6).

In summary, with the increasing demand for durability design in RC structures the use of thick concrete cover is introduced in practice. It is therefore useful to understand the mechanics of RC members with thick cover and predict their behavior. The existing widely accepted models for torsion are developed based on the database only concentrated for members with relatively small cover and fail to capture the torsion behavior of RC members with a relatively thick cover. Furthermore, the available spalling theories cannot fully explain the physically observed spalling behavior and lack generality of application. In this paper, by using the recently conducted pure torsional experiments on nine RC specimens with varying concrete cover, transverse rebar, and concrete strength, a critical assessment of the state-of-the-art models is conducted. Later, a new rational theory for the spalling of concrete cover which can be integrated into existing theoretical models is forwarded.

2. Torsional experiments on RC beams with thick concrete cover

While adding to the handful database in the domain of thick cover, recently an experimental program was undertaken to better understand the mechanics of torsion of RC members with relatively thick concrete cover [7]. The specimen designation with sectional detailing is given in Table 1and Fig. 5.

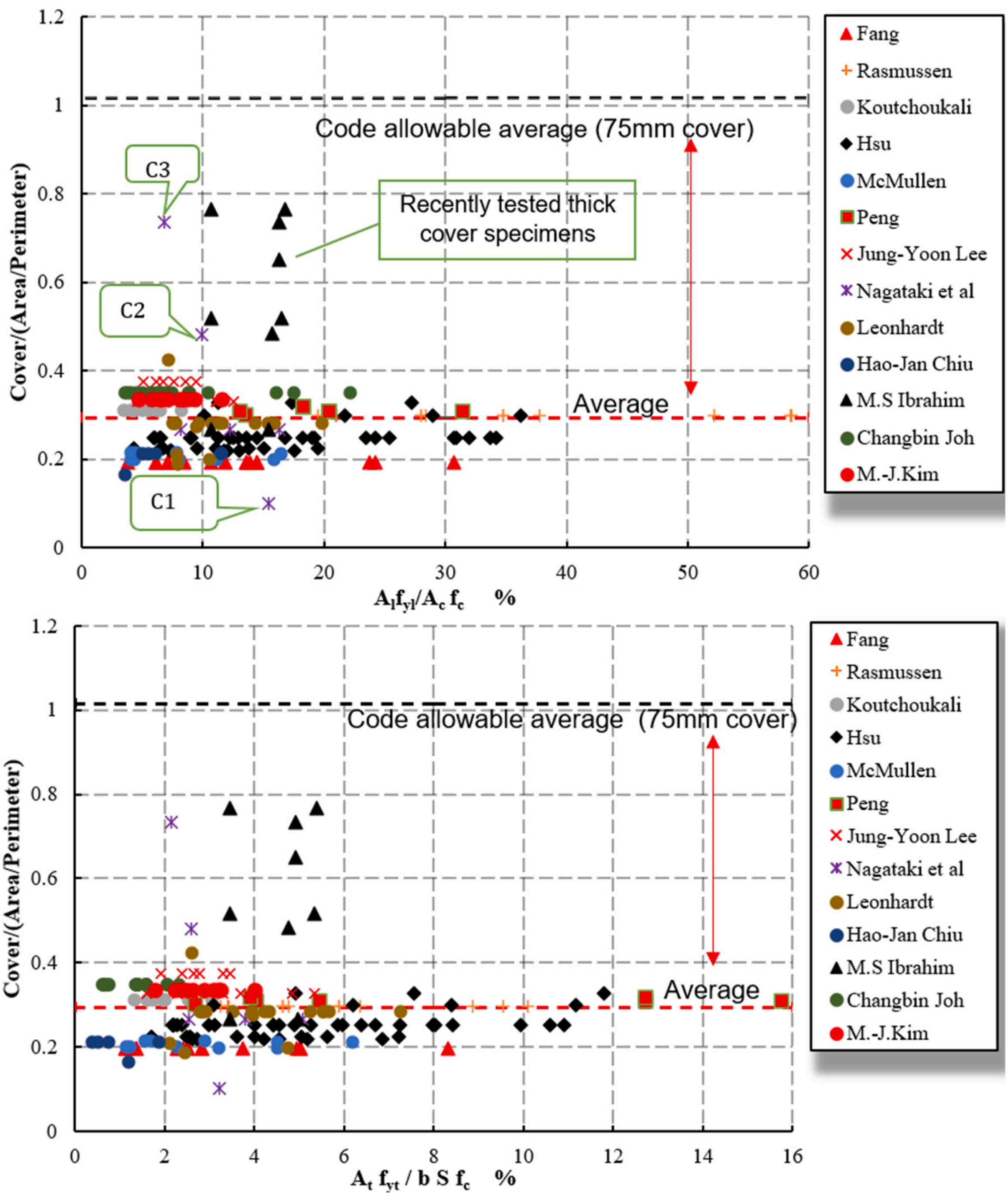

Fig. 2. -Experimental researches pertaining to concrete cover against reinforcement ratio.

Fig. 3. Torsional failure of a member showing significant spalling of concrete cover [7].

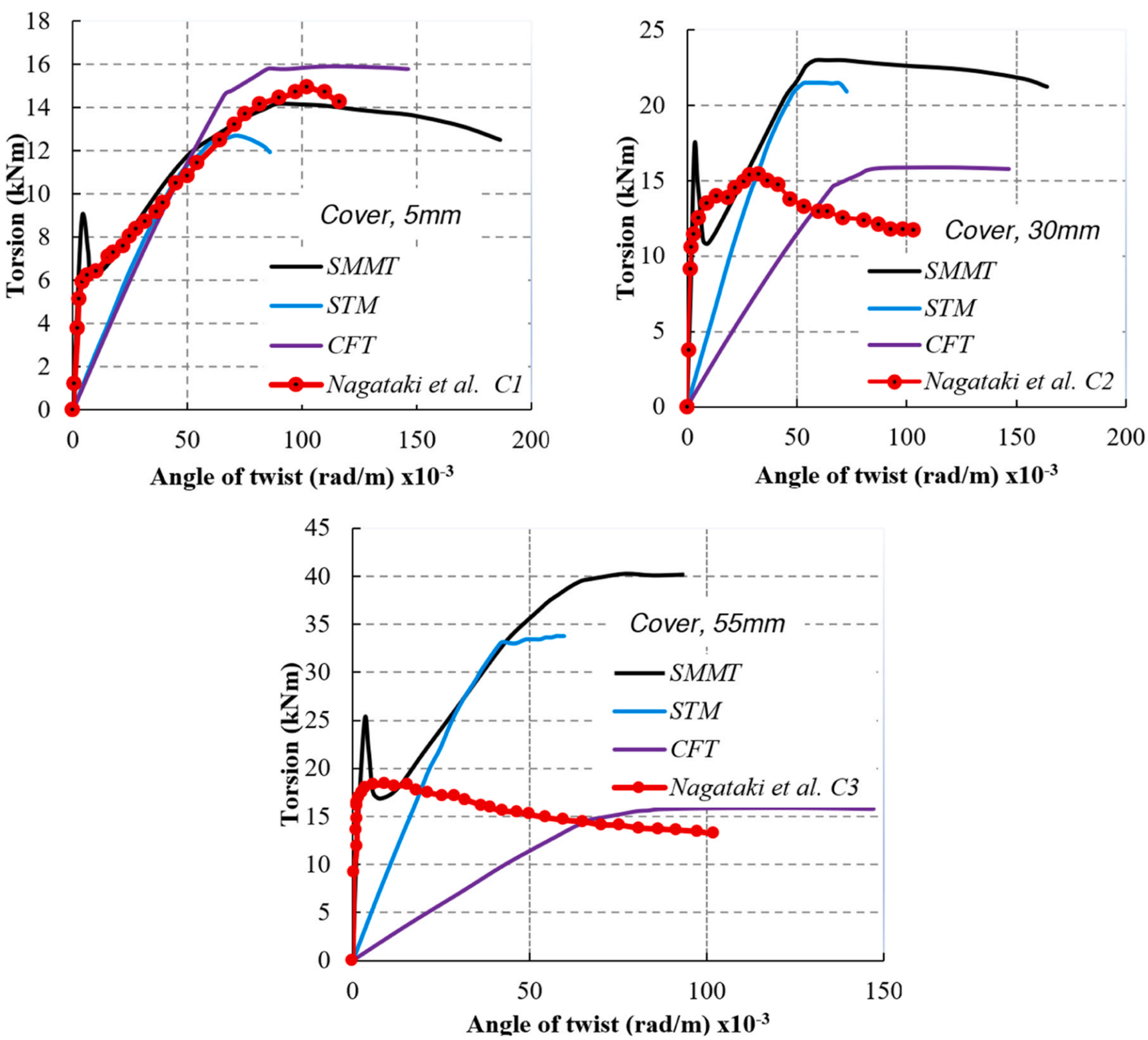

Fig. 4. Models comparison with the experiment by Nagataki et al. (Cover is from surface to centerline of transverse reinforcement).

Table 1
Specimen designations with cross-sectional and mechanical properties [7].

Set	Designation	Clear cover (mm)	A_l (mm^2)	A_t/S (mm)	f_{yl} (MPa)	f_{ul} (MPa)	f_{yt} (MPa)	f_{ut} (MPa)	f_c (MPa)	f_{ct} (MPa)
1	NSC-S1-C30	16	452.39	0.628	689.7	817.4	534.1	659.5	42.1	3.8
	NSC-S1-C45	31	452.39	0.628	689.7	817.4	534.1	659.5	39.4	3.7
	NSC-S1-C60	46	452.39	0.628	689.7	817.4	534.1	659.5	38.8	3.5
2	NSC-S2-C45	29	452.39	0.604	689.7	817.4	521	647.1	41.4	3.5
	NSC-S2-C55	39	452.39	0.604	689.7	817.4	521	647.1	39.9	3.5
	NSC-S2-C60	44	452.39	0.604	689.7	817.4	521	647.1	40	3.4
3	HSC-C30	16	452.39	0.628	689.7	817.4	534.1	659.5	60.8	5.1
	HSC-C45	31	452.39	0.628	689.7	817.4	534.1	659.5	60.8	4.6
	HSC-C60	46	452.39	0.628	689.7	817.4	534.1	659.5	60.8	4.3

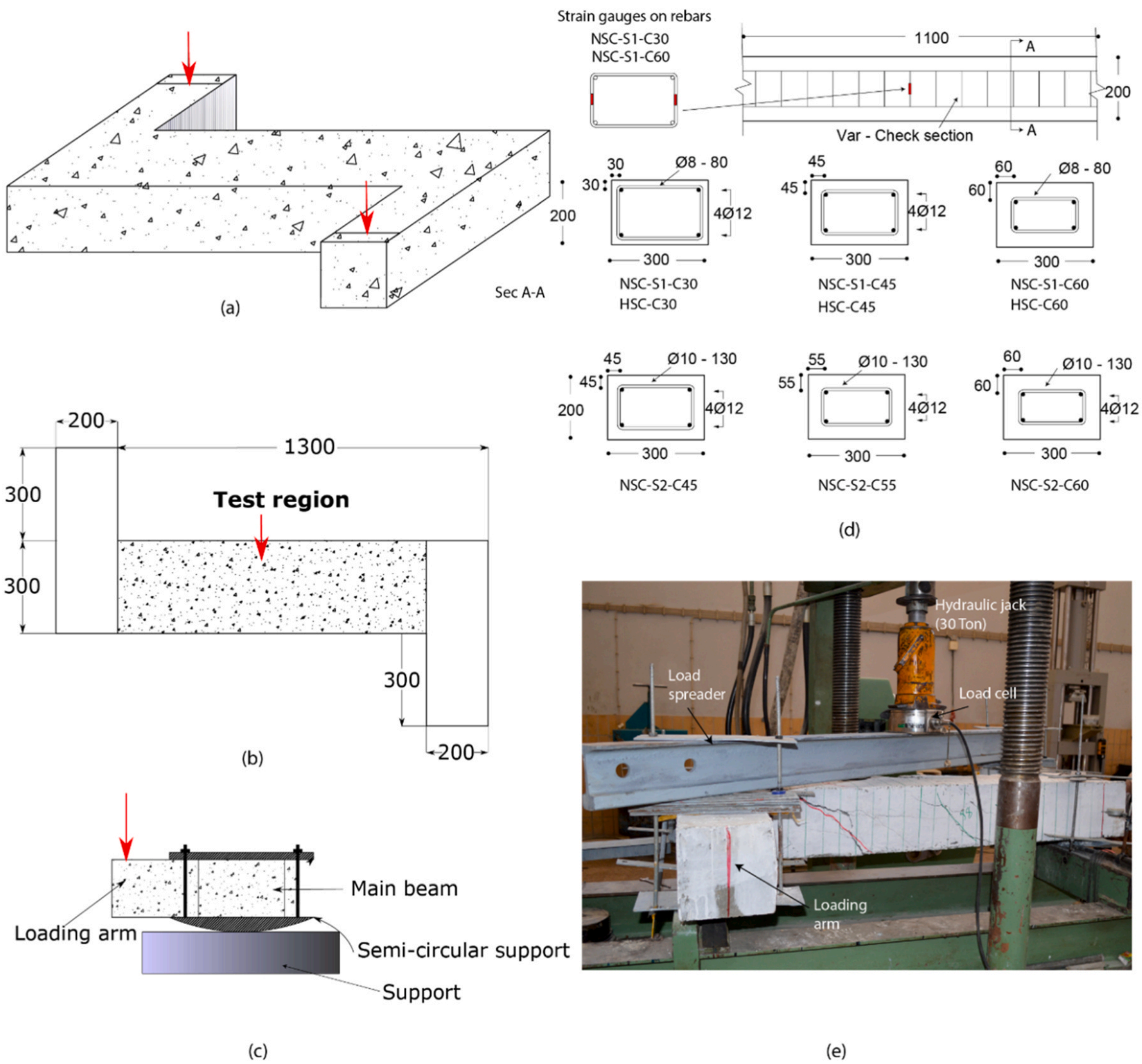

Fig. 5. Test set up (a) 3D view of the specimen (b) Top view and test region (c) detail of support condition (d) Detailing of the specimens (all dimensions are in mm) (e)Specimen during testing [7].

3. Evaluation of existing theoretical models for thick cover

3.1. Experimental result

The torsional behavior of the specimens is presented in Fig. 6 and Table 2. The specimens with relatively small cover showed a linear and very stiff behavior up to the cracking torsional capacity. After the formation of diagonal cracking, the specimens (NSC-S1-C30 and HSC-C30) exhibited an increasing post cracking capacity with softened torsional stiffness. The remaining specimens with large concrete cover after reaching their corresponding cracking load, due to significant cover spalling their behavior shows a decline in load-carrying capacity. Hence, the peak capacity of the specimens with large cover coincided with their corresponding cracking capacity. Moreover, the ultimate capacity of the members is controlled by the spalling of the concrete cover (see Fig. 7).

Generally, the specimens with relatively small concrete cover failed due to the crushing of the softened diagonal strut coupled with concrete cover spalling. The cover spalling initiated after the cracking torsion and the spalling was restricted to the edge of the member. In contrast, for the remaining members with thick cover, the specimens failed prematurely

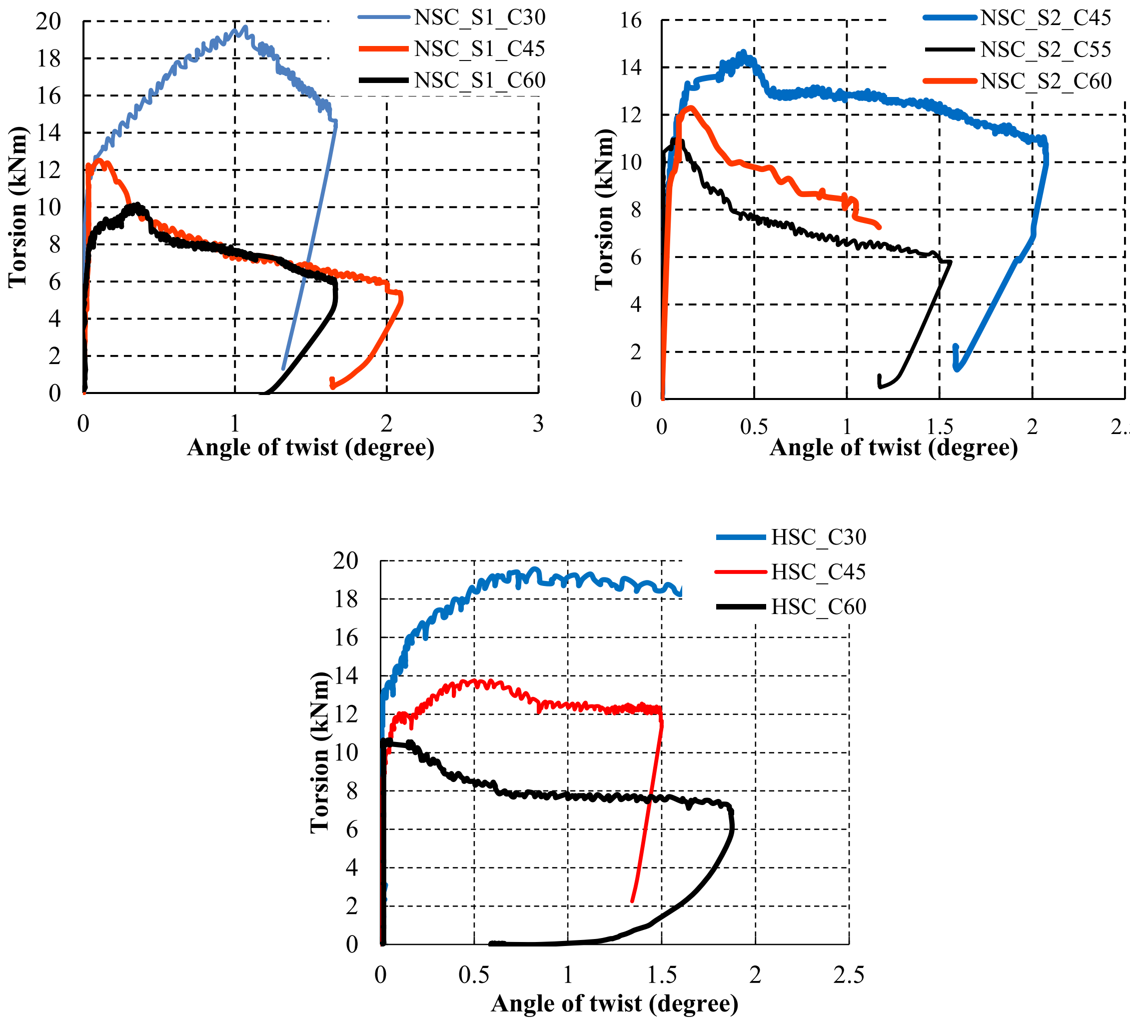

Fig. 6. Experimental result [7].

Table 2
Experimental result [7].

Set	Designation	T_{cr} (kNm)	T_{ult} (kNm)	Failure Mode
1	NSC-S1-C30	11.2	19.71	Crushing of strut accompanying with spalling* of concrete cover
	NSC-S1-C45	10.8	12.51	Spalling of concrete cover
	NSC-S1-C60	8.2	10.15	Spalling of concrete cover
2	NSC-S2-C45	12.8	14.66	Spalling of concrete cover
	NSC-S2-C55	10.8	10.95	Spalling of concrete cover
	NSC-S2-C60	11.4	12.25	Spalling of concrete cover
3	HSC-C30	13.6	19.86	Crushing of strut accompanying with spalling* of concrete cover
	HSC-C45	11.6	13.76	Spalling of concrete cover
	HSC-C60	9.4	10.65	Spalling of concrete cover

$\mathbf{T_{cr}}$ visible crack observed *The spalling was limited to the edge of the member

due to spalling of concrete cover. The spalling affects essentially the full perimeter of the member. Furthermore, the initiation of the spalling commenced near the diagonal cracking torsion. Detailed observations and comprehensive comparison of the experiments with commonly used codes and advanced graphical methods can be found from the original work [7].

3.2. *Comparison of the theoretical models with thick cover experiments*

The modern truss models for torsion are built on the Navier principle of mechanics. These models can be used to predict the full torsional response of RC members subjected to pure torsion [5,27,28]. They are extensively tested with a large number of experiments providing a consistent prediction which led to the development of simplified models and equations based on the theories [35–37]. A comparison between the experiments and the prediction by SMMT, STM, CFT is made using the recent group of experiments [7] to evaluate the capability of the models. The specimens failed due to a localized spalling of concrete cover over a finite length (See Fig. 3 and Fig. 7). Further measurements showed the length of the spalled region is essentially equal to the larger side dimension. Michell and Collins [5] also observed the localized effect and noted '*The concrete cover will not spall-off over the entire length of the beam*'. In the current investigation of specimens with thick cover, the total observed rotation after cracking/spalling is essentially concentrated to the finite spalled region. In the following analysis, to directly compare the results with the model's prediction, the total angle of twist is calculated considering the finite spalled length of 300 mm.

The comparison between SMMT, STM, and CFT with the different cover experiments is presented in Fig. 8. The models closely predicted the behavior of the specimen with a relatively small cover (NSC_S1_C30). The specimen failed due to the crushing of the diagonal

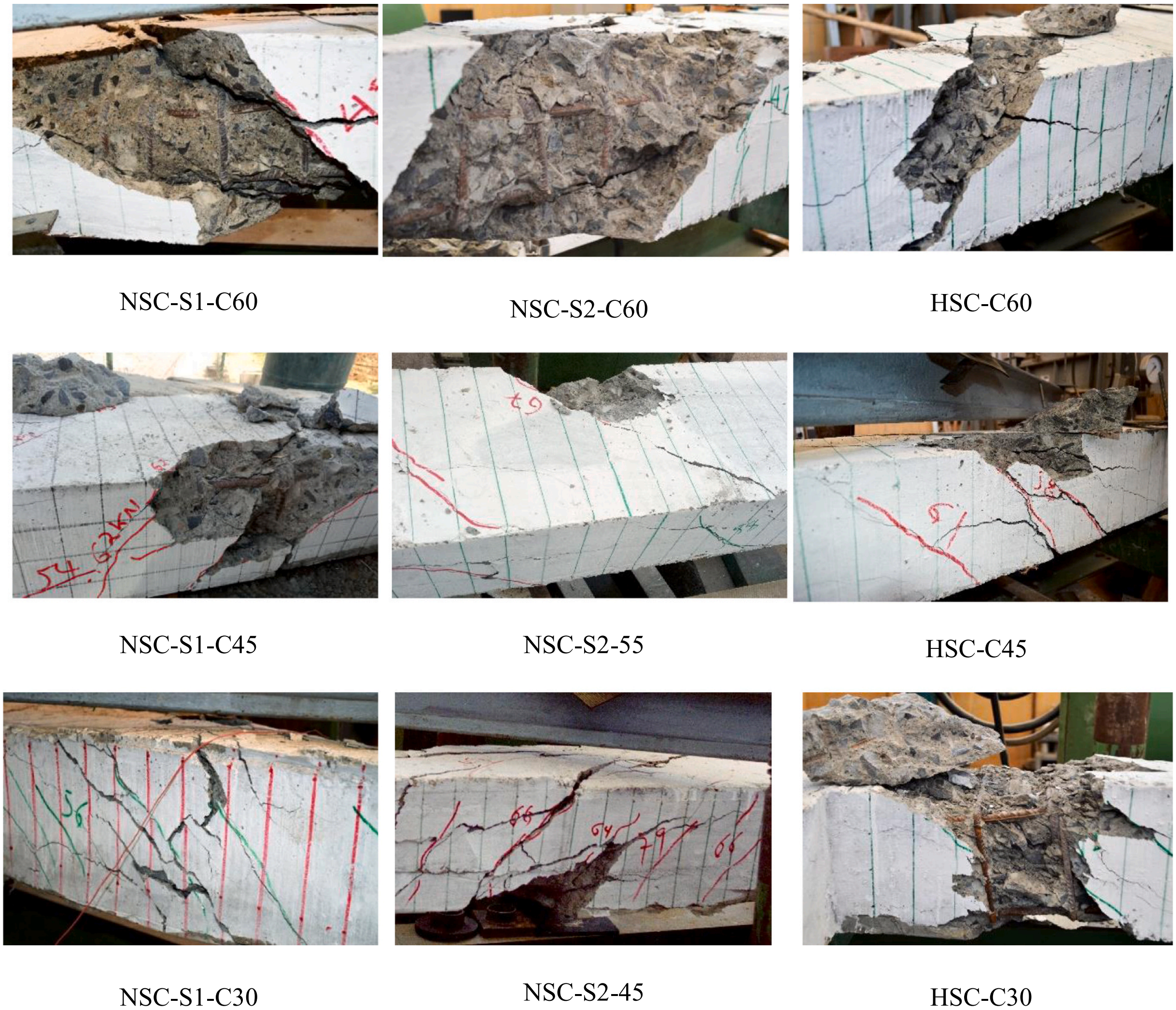

Fig. 7. Specimen failure due to significant cover spalling (Specimens NSC-S1-C60, NSC-S2-C60, HSC-C60, NSC-S1-C45, NSC-S2-C55, HSC-C45 and NSC-S2–45) and crushing of strut accompanied with spalling of concrete (NSC-S1-C30, HSC-C30).

strut coupled with concrete cover spalling. The spalling of the cover was limited to the edge of the member and initiated after the cracking torsion. STM predicted the peak capacity with greater accuracy whereas CFT and SMMT slightly overestimated the ultimate capacity.

For Set1 and Set2 beams with relatively thick cover, STM and SMMT couldn't able to provide an adequate prediction. The specimens were having a clear cover of 31 and 46 mm and failed due to concrete cover spalling. The spalling of the concrete cover occurs around the cracking torsion. Contrary to the experiment, SMMT predicted an enhanced post-crack capacity in which the peak capacity is controlled by concrete crushing of the strut. Similarly, STM predicted a highly overestimated strength with the specimen failing by the crushing of diagonal strut. Generally, both SMMT and STM highly overestimated the peak capacity of the specimens.

Comparing the experiments with CFT, the peak capacities are adequately captured. However, the model highly overestimated the twisting behavior (predicting large twist at peak). In the experiment, the peak capacity of the members with thick cover was observed near the cracking torsion which is a fraction of the models' prediction.

The last set of specimens (Set 3) were cast from concrete with relatively higher compressive strength. All the models slightly overestimated the peak capacity of the specimens with the small cover. For the specimens with large cover, the failure behavior is erroneously predicted by SMMT and STM and additionally, the peak capacity of the members is highly overestimated. Similar to the previous sets, CFT erroneously predicted the peak capacity to have coincided with a large angle of twist.

Observing the above comparisons, while the models (STM and SMMT) could provide an excellent prediction for specimens with smaller cover, the models were not able to provide adequate prediction to specimens with relatively large cover. Both models ignore failure due to spalling of cover and inherently assume failure to be controlled by concrete strut crushing or rebar rupture regardless of the thickness of the cover concrete. Nevertheless, for specimens with large concrete cover, the peak capacity of members may be controlled by the spalling of cover concrete.

Opposite to the above models, CFT considers concrete cover spalling and provides a safe estimate. However, the prediction of the twist behavior and failure mode is not satisfying. Moreover, the model uses a spalled section for the analysis of torsional members. While it is true that cover spalls during torsional actions, initiation of spalling of concrete cover is not addressed in the model. For members with small cover, cover spalling may initiate after the cracking torsion near or after the peak capacity of the member. While for members with large cover, spalling of concrete cover commence near the cracking torsion. Thus, using a spalled section throughout the analysis cannot be physically explained.

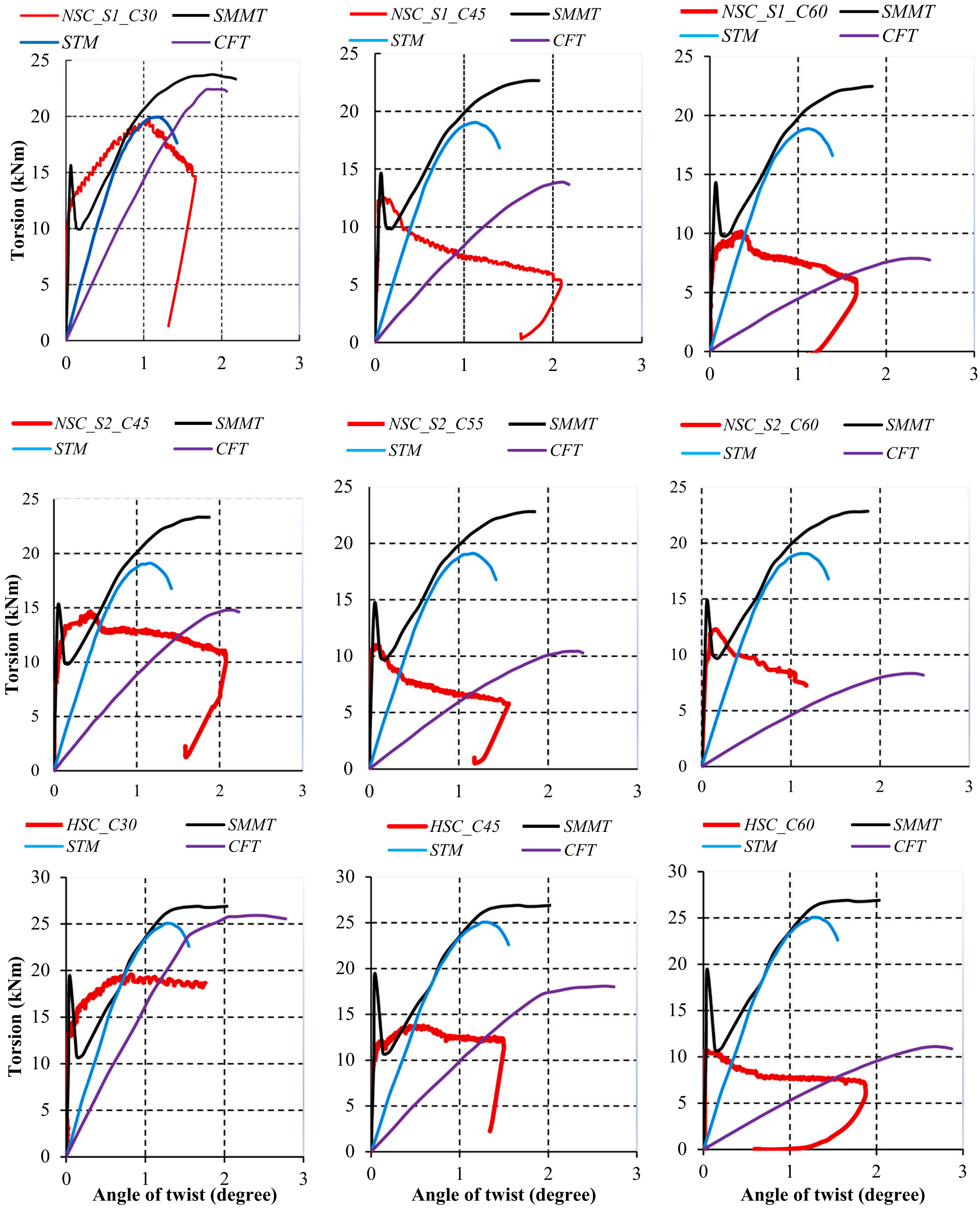

Fig. 8. Comparison between the experiments and the prediction by SMMT, STM, CFT.

4. Mechanics of spalling of concrete cover

Failure is linked with concrete crushing or rebar rupture in RC members subjected to flexure. In addition to these modes of failure, a torsional member might prematurely fail due to concrete cover spalling. Although rigorous studies resulted in a better understanding of the mechanics of torsional strength and failures associated with strut crushing and rebar rupture, the mechanics of concrete cover spalling does not have a unified consensus. The lack of consensus on the effect of concrete cover can be observed by comparing the torsional resistance prediction of different models and codes [16,17,35,36,38,39] (See Fig. 9). For the given section, the only variable was the cover concrete. The disparity in the torsional resistance by the models and codes gets more pronounced with the increase of cover. The comparison (see Fig. 8 and Fig. 9) between experiment, codes, graphical methods, and advanced torsional models clearly show an absence of consensus on the role of cover concrete for RC members under torsional actions. The disparity indicates and validates the need for a thorough examination of

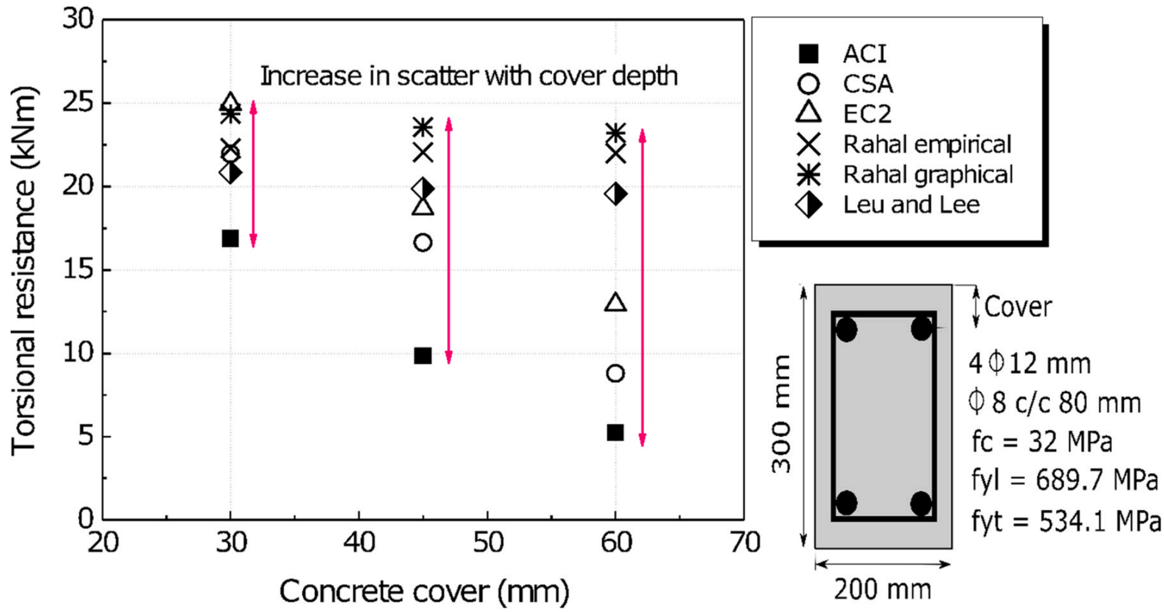

Fig. 9. Torsional resistance prediction of different models and codes [16,17,35,36,38,39].

the impact of concrete cover.

Regarding the experimental investigations, there are very limited studies on the effect of concrete cover [7]. The limited studies which gave a thorough insight on the concrete cover include the study by Mitchel and Collins [5] during the formulation of the CFT model, Rahal and Collins [6,30] on their study on the combined shear and torsion, and

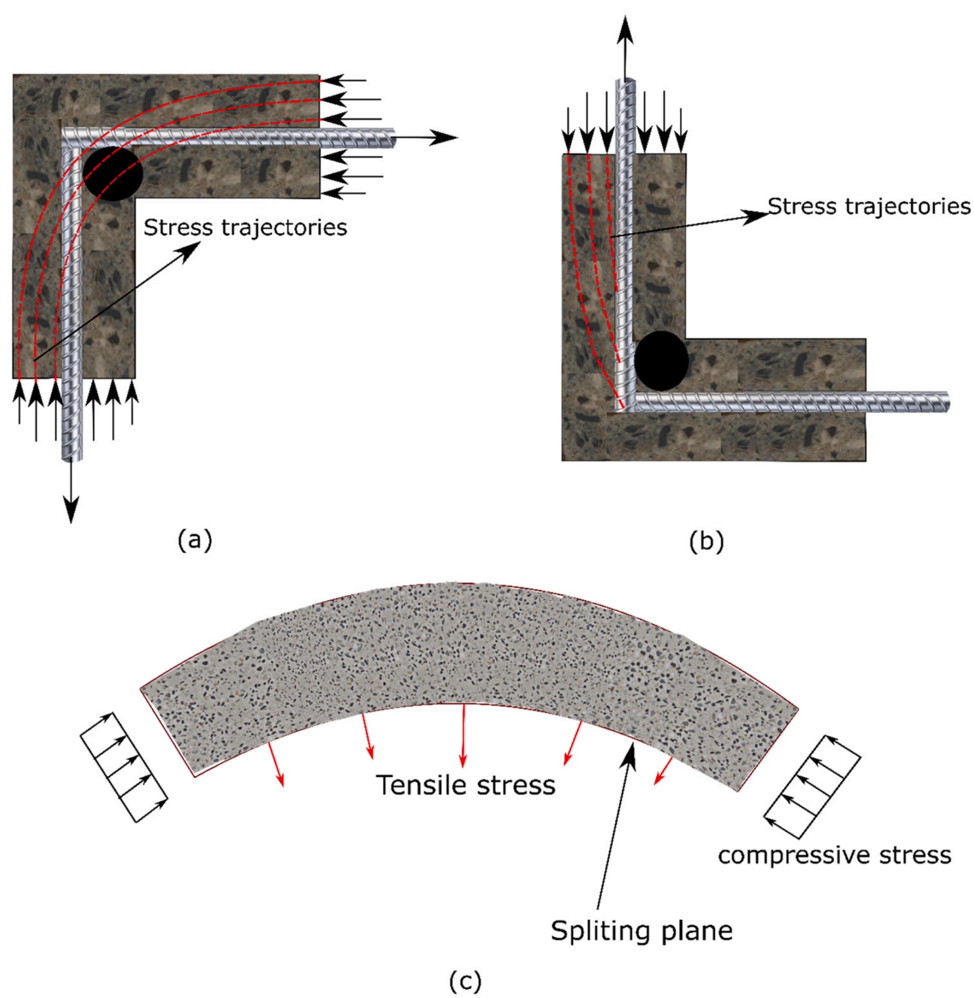

Fig. 10. Spalling of concrete cover models (a) Mitchell and Collins [5] (b) Fisher et al. [42] (c) Rahal and Collins [30].

a recent investigation of shell element by Bruun and Bentz [40].

Mitchell and Collins [5,26] proposed a CFT model for members subjected to torsion and shear. In their investigation, they observed the spalling of cover. Mitchel and Collins noted that '*the compression in the concrete tends to push-off the corner while the tension in the hoops holds it on. As it will not be possible for the hoops to hold on the concrete cover without generating large tensile stresses in the concrete, at higher loads this cover will spall off.*' (See Fig. 10a).

Similar to the assumption of the CFT model, Rahal and Collins [6,30] assumed a mechanism of spalling of cover to be due to the tensile stress developed by the change in the direction of compressive stress (See Fig. 10c).

In general, both the studies by Mitchell and Collins [5] and Rahal and Collins [41] attributed the spalling of concrete cover with the change in direction of compressive stress trajectory. Although the assumption is reasonable for members subjected to torsion, the theory could not fully explain the spalling of concrete cover for members subjected to shear. Fisher et al. [42] observed spalling of concrete cover on members subjected to shear. Like torsional spalling, the authors associated the spalling phenomenon with the change in direction of the diagonal compression stresses as they approach the corner of the member (see Fig. 10b). The described phenomenon cannot fully explain the observation since severe cover spalling is also observed at the mid-section of the members. Contrary to the *change in direction of the* corner stress field, the diagonal stresses around the mid-section are parallel to the surface. Therefore, it is not anticipated they will cause the cover to spall.

Recently Bruun and Bentz [40] conducted the first pure torsion test on shell elements. The shell element has a square dimension of 1626 mm and a thickness of 285 mm. Two specimens were cast with and without out of plane rebar and with similar in-plane reinforcement. The experimental investigation showed both specimens exhibited spalling of concrete cover.

The experiment showed a clear separation of the cover. Like the spalling due to shear in beams, the assumption of spalling of cover initiated from the edge element fails to explain the observed spalling on the shell element. A closer investigation of the surface deformation reveals that the compression trajectory due to torsion is inward which is contrary to the assumption of Rahal [30]. Since the observed compression trajectories are opposite to the assumption of Rahal's model, the stress on the failure plane will be compression rather than tension.

Without Doubt, the studies by Mitchell and Collins [5] and Rahal and Collins [30,41] greatly enhanced the knowledge on the torsion of RC members. Yet, the assumed mechanics of spalling cannot fully explain the physically observed behavior. The limitation of spalling theories can be observed in the lack of generalizability. While the assumptions appear adequate for linear torsional members (beams), the theories cannot fully explain spalling due to shear and spalling of cover on shell elements. In general, the torsion of RC members has been extensively investigated for the past 60 years, so far, the mechanics of the spalling of concrete cover is not fully understood.

5. Proposed spalling mechanism

When RC members are subjected to torsion a circulatory shear stress will occur. After cracking, the member may be treated as composed of equivalent wall (panel) elements (See Fig. 11).

A closer investigation of one of the wall panel elements is shown in Fig. 12a. The wall panel element bounded by the rebar cage and the outer surface is further isolated. The resulting element is subjected to in-plane shear stress due to the acting torsional moment. The acting uniform shear stress will create an in-plane shear flow q_c and torsion T_c on any plane which is perpendicular to the shear stress plane (see Fig. 12b). For RC members with longitudinal and transverse rebar, due to the mere presence of the rebar cage, the surface along the rebar grid will be relatively weaker. And once the limit (resistance) is exceeded on the weaker plane, the acting in-plane shear and torsion on the critical plane will result in spalling of the concrete cover.

More conveniently, the effect of the acting in-plane shear and torsion on the weaker plane can be observed by rotating the in-plane actions by 45 degrees. The resulting stress condition on the critical surface will be equivalent bending in the orthogonal directions (see Fig. 12c). It is also interesting to note that the orientation of bending moments on the critical surface is consistent with the physically observed spalling direction. The acting spalling moment per unit width will be a function of

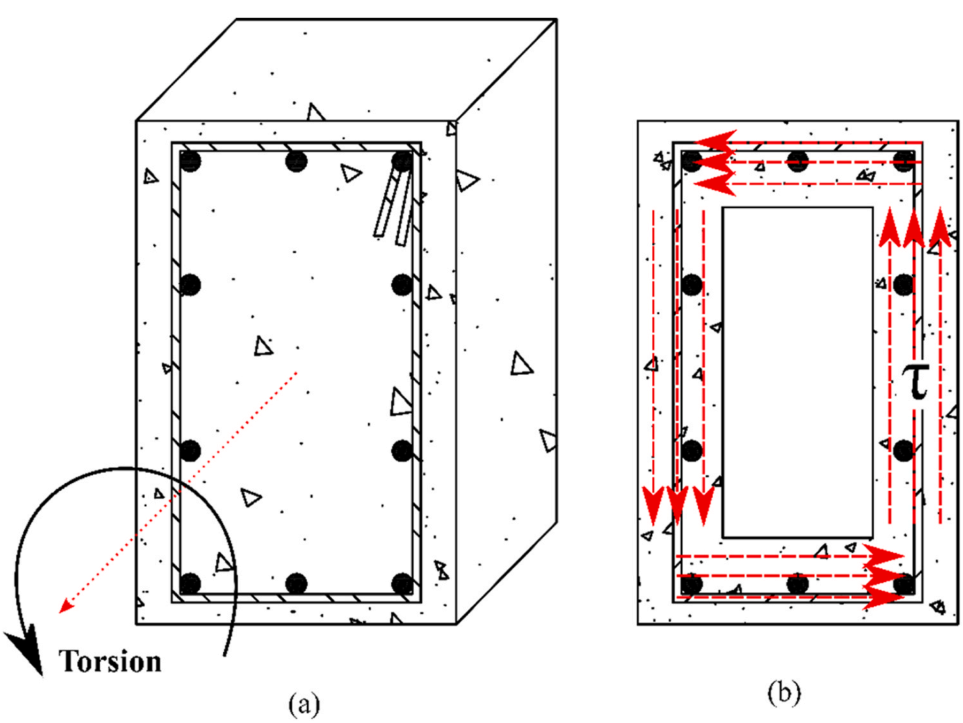

Fig. 11. (a) RC members under torsional action (b) equivalent wall panel element subjected to shear stress.

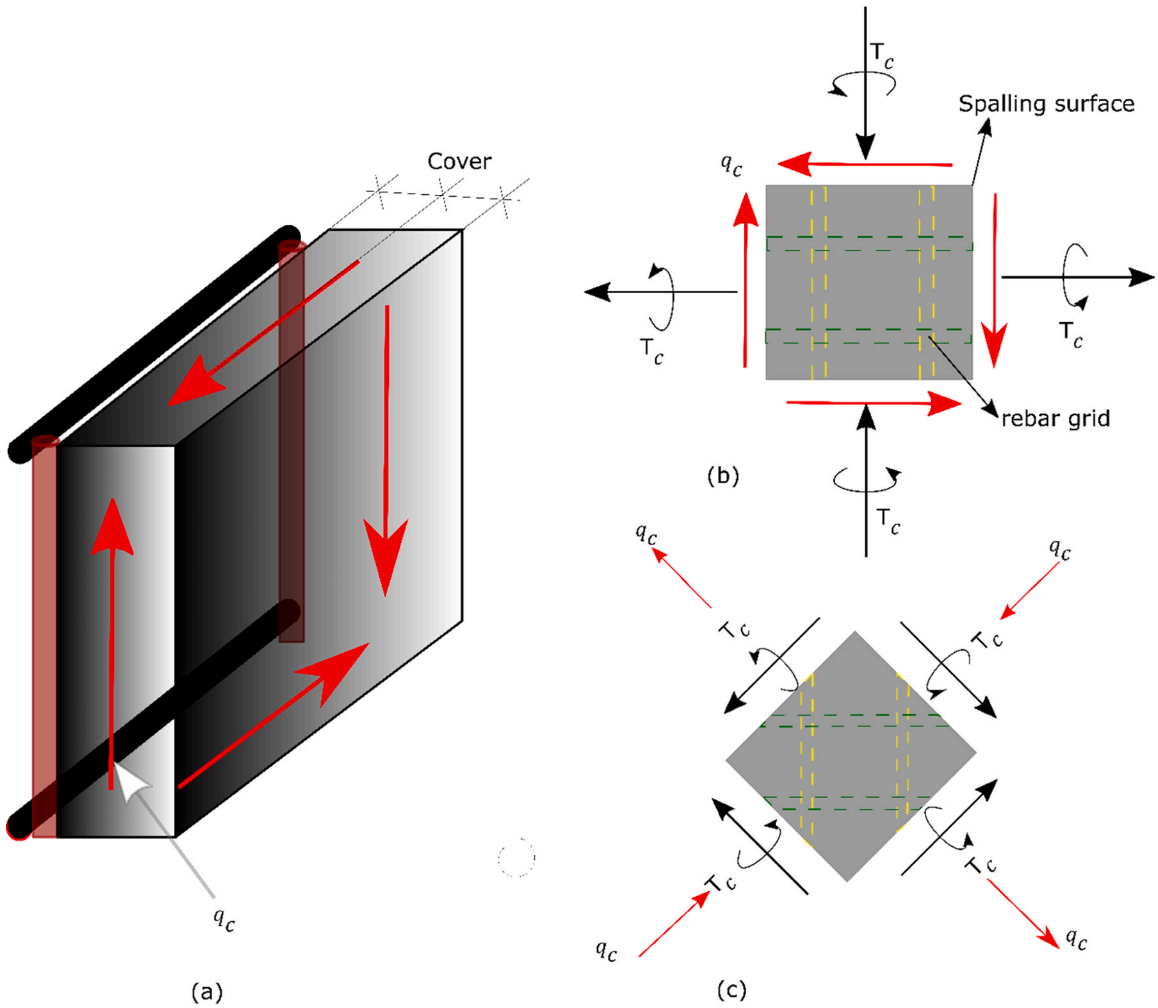

Fig. 12. (a) wall panel element subjected to in-plane shear stress (b) in-plane shear and Torsion on the plane of weakness (c) Equivalent bending in the orthogonal direction.

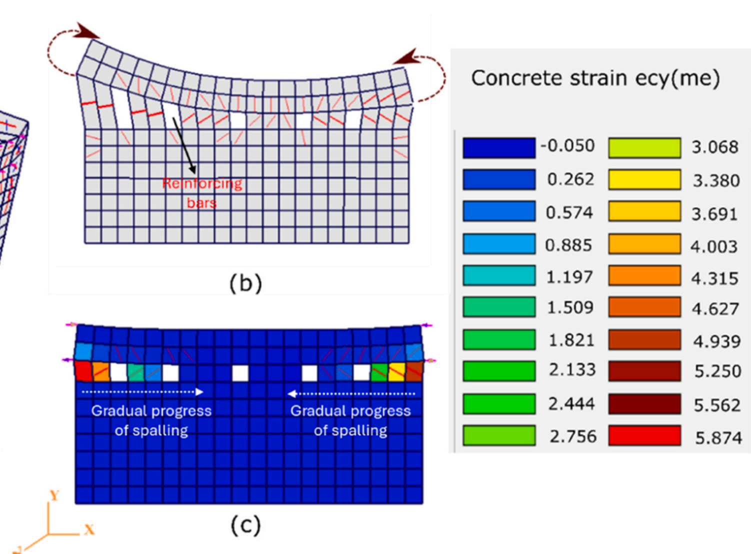

Fig. 13. (a) Cover under a spalling diagonal moment (3D) (b) crack propagation (2D) (c) tensile strain along the spalling direction (Spalling evolution).

shear stress and thickness of cover and will have a magnitude given by Eqs. 1 and 2.

$$q_c = \left\{ \begin{array}{ll} \tau \ C_C & t_d \geq C_C \\ \tau \ t_d & t_d < C_C \end{array} \right\} \tag{1}$$

$$T_c = \left\{ \begin{array}{ll} q_c \dfrac{C_C}{2} & t_d \geq C_C \\ q_c \left(C_C - \dfrac{t_d}{2} \right) & t_d < C_C \end{array} \right\} \tag{2}$$

Where C_C: Clear cover.

t_d: Thickness of shear flow zone.

Generally, the diagonal bending stress which resulted from the torsional moment is responsible for spalling. The presented approach of spalling is consistent and fully applicable for the spalling of cover on beam in shear. The only modification will be the acting shear stress will be due to shear force rather than circulatory shear stress due to torsion.

Cover spalling initiation is mainly dependent on the thickness of the concrete cover, discontinuity created by rebar, and tensile strength of the concrete. The initiation and evolution of concrete cover spalling are a gradual process. The gradual evolution of the spalling process due to the spalling diagonal moment can be observed by conducting a nonlinear finite element analysis (NLFEA). Presented in Fig. 13 is a detailed NLFEA of an isolated concrete element bounded by the surface and the core concrete. The nonlinear analysis is conducted using a three-dimensional finite element package VecTor 3 [43]. The isolated concrete element is loaded with gradually increasing diagonal spalling moment in the orthogonal directions, see Fig. 13a.

As it can be seen from the analysis, the spalling started at weak zones, which usually are located on the plane where the rebars are located, and gradually progresses to the remaining zone, see Fig. 13b and Fig. 13c. The spalling due to diagonal moment assumption is also further examined with a recent flexure experiment on a U-shaped member (See Fig. 14). The flexural moment is applied through two loading wings. The U-shaped specimen was cast from lightweight concrete having a compressive strength of 24 MPa and tensile strength of 1.7 MPa (See Fig. 14). The specimen was reinforced with rebar in the flexural tensile zone. The specimen was loaded to 60 % of its ultimate capacity and the applied load was maintained for 10 days. In addition to flexural tensile cracks, due to the relatively smaller tensile strength, a splitting crack which is similar to spalling was observed. During the days following the initial splitting, a propagation of the spalled layer was observed (see Fig. 14). Although there was no apparent weak plane owing to the rebar cage, due to the absence of a strong aggregate interlock, a local weak plane was present. Consequently, the observed spalled layer was created. Furthermore, it should be noted that the member was essentially subjected to similar boundary conditions with that of concrete cover under the diagonal spalling moment.

5.1. Spalling strength (threshold)

The acting diagonal spalling moment acts on surfaces that are perpendicular to the shear stress plane. Due to the mere presence of the rebar grid, the surface just above the rebar grid will be a weaker plane. Thus, the spalling of concrete cover will initiate once the spalling resistance of the weak plane is exceeded by the corresponding acting diagonal spalling moment.

The actual stress distribution during the spalling evolution is complicated. The link between the tensile stress variation on the spalling surface and the thickness of concrete cover was investigated by conducting a nonlinear finite element analysis. The investigation showed the gradual evolution of spalling and more interestingly the correlation between the thickness of cover and effective width of the tensile stress on the spalling surface. During the spalling evolution, the effective width of the tensile stress zone was essentially equal to the cover thickness. Taking a cover thickness of 20 and 40 mm, Fig. 15 shows the correlation between the thickness of the cover and the tensile stress zone. The gradual evolution of the resisting tensile stress for different levels of delamination is also presented in the plot.

The spalling resistance of RC members is mainly dependent on the tensile strength of the concrete, concrete cover thickness, and the rebar grid. The spalling resistance can be derived by considering the equilibrium requirement at the initiation of spalling between the acting spalling moment and resistance offered by the tensile strength of the concrete (See Fig. 16a-c). Since the effective width of the tensile stress zone is dependent on the concrete cover thickness, the effective width of three-fourth of the cover thickness is used in the current formulation. The reduced effective width is implemented to account for the tensile stress

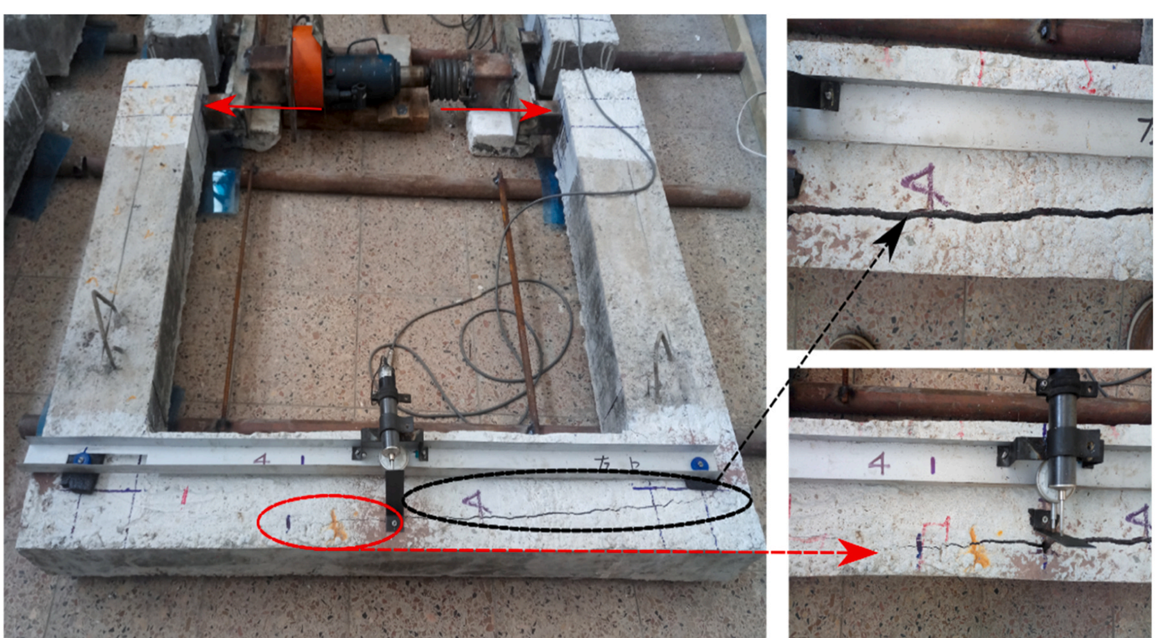

Fig. 14. Splitting crack propagation.

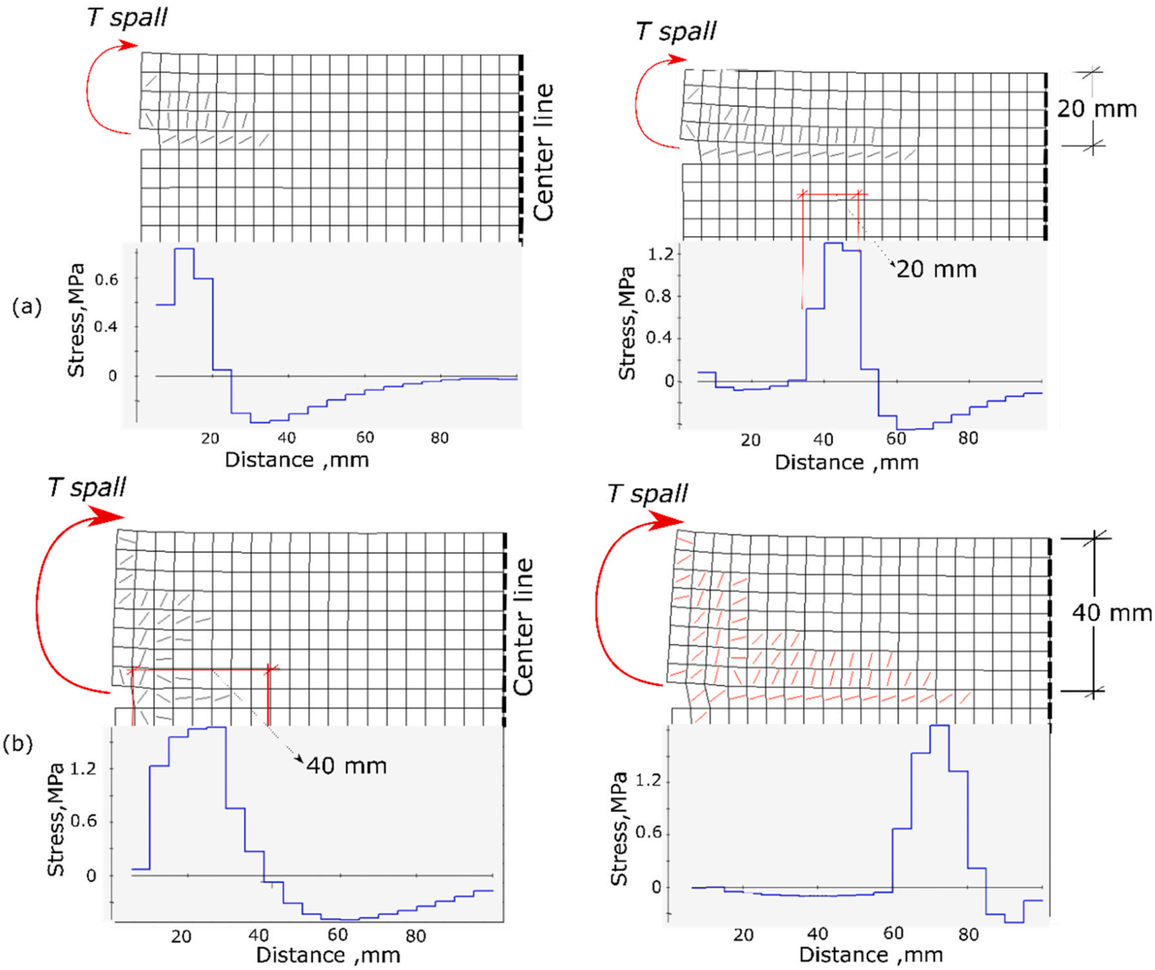

Fig. 15. Evolution of cover spalling (a)20 mm cover (b) 40 mm cover.

variation within the effective width and also incorporated to address the slight positive contribution of the compressive stress zone. Incorporating the effective width, the spalling resistance of the critical plane is derived and given by Eqs. 3 and 4.

$$T_{spall} = \begin{Bmatrix} \frac{3}{8} f_{ct} C_c \left(Z - \frac{3}{4} C_c \right) & Z > 1.5 C_c \\ \frac{1}{8} f_{ct} Z^2 & Z \le 1.5 C_c \end{Bmatrix} \quad (3)$$

$$\text{Where } f_{ct} = 0.31\sqrt{f_c}$$

$$Z = \max \begin{Bmatrix} \min\left(\frac{b}{\sin\theta}, \frac{S - 2\phi_s}{\cos\theta} \right) \\ 2\left(\frac{C_C - \frac{\phi_l}{2}}{\sin\theta} \right) \end{Bmatrix} \quad \text{Where } \theta = 45^\circ\ b$$

$$= height - 2C_c - 3\phi_l \quad (4)$$

In the spalling resistance formulae, the spalling capacity is a maximum of the spalling resistance offered by the region between the rebar cage and the section outside of the grid (see Fig. 17). For members with smaller cover, the spalling strength is governed by the resistance due to the section within the rebar cage (see Fig. 17a), whereas for large cover, the spalling resistance is controlled by the strength of the outside region (see Fig. 17b). In the formulation, the effect of the discontinuity created by the rebar grid is accounted for by considering an apparent length for spalling resistance '***Z***'. Furthermore, the concrete sections within half the rebar diameter distance are assumed to not contribute to the spalling resistance due to the bond deterioration effect (see the red zone in Fig. 17).

Generally, by observing the acting spalling moment and spalling resistance equation derived in the above formulations, the proposed spalling model inherently assumes members susceptibility to spalling of cover concrete to be governed by, the thickness of the concrete cover, tensile strength of concrete, presence of rebar cage and their location, and size of the member.

5.2. Application of the spalled model

In RC members, contrary to the most common assumption of the identical response of the side and top/bottom panels used in advanced models [5,27,28] (See Fig. 18a), pure torsional experiments on members with higher aspect ratio indicates varying response between the shorter and longer sides [12]. Because of this non-uniform behavior of adjacent panels, concrete cover spalling on the different faces will not commence at the same instant. There is a gradual spalling initiation and evolution on the short and long side mainly dictated by the applied shear stress, rebar arrangement, and cover thickness. Thus, to mitigate the deficiency of using a single membrane element torsional modeling, the SMMT is further extended to model the varying behavior of the four panels of rectangular RC members. For members with symmetrical longitudinal reinforcement arrangement, the response of the opposite panels is identical. As such, the pure torsional behavior of the members can be described by considering two adjacent panels namely the side and top or bottom panel.

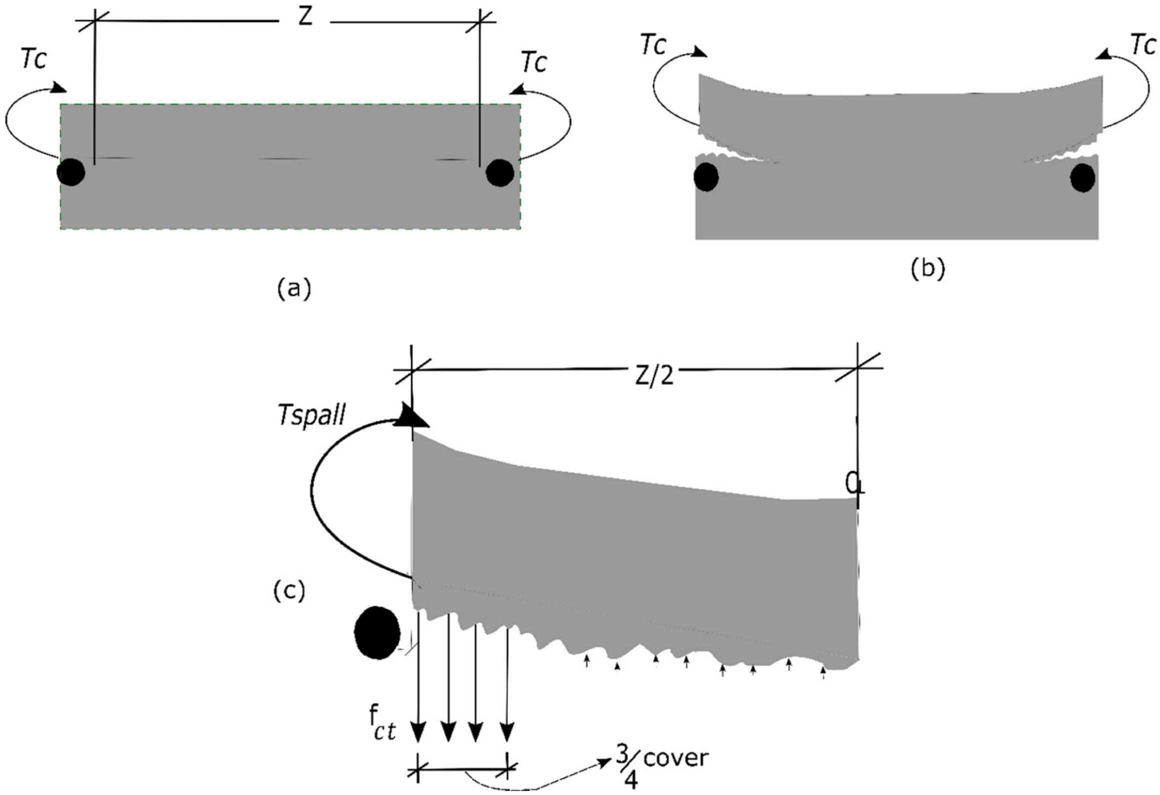

Fig. 16. (a) Concrete cover under a spalling moment (b) gradual spalling (c)Spalling resistance at the initiation.

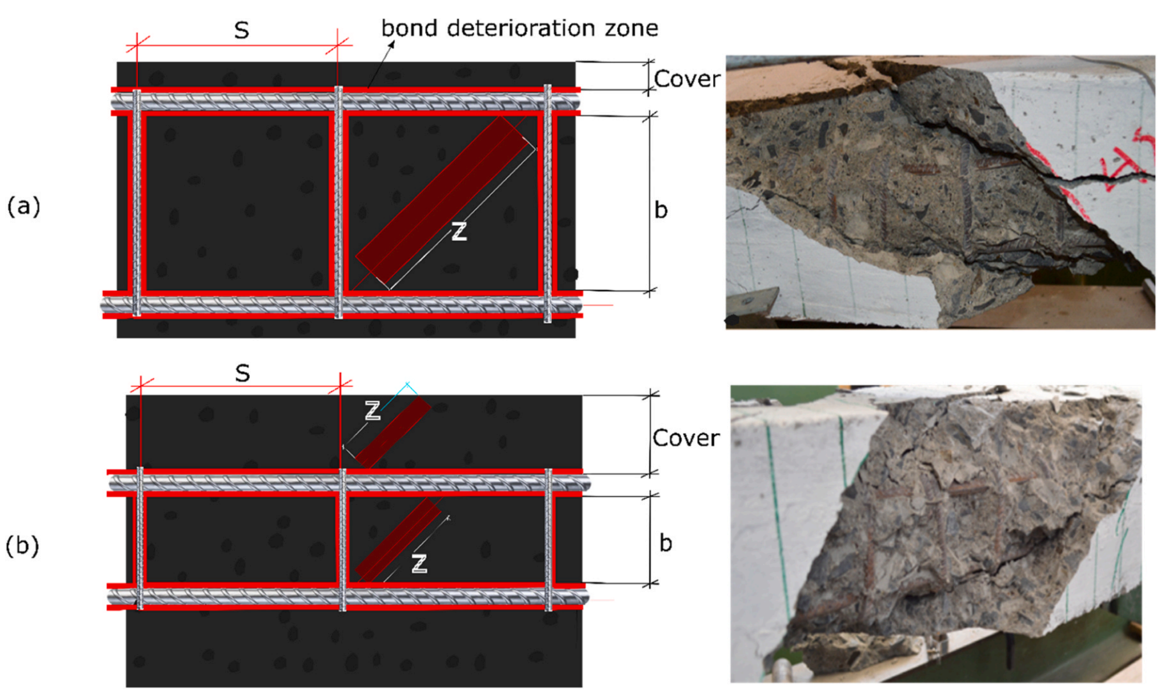

Fig. 17. Regions of spalling resistance for small and thick cover (a) small cover (b) Thick cover.

In the proposed approach, with some adjustments, the individual panel elements are analyzed using the equilibrium, compatibility, and material models of the softened membrane model for torsion. While consistent and excellent predictions can be found from the single membrane modeling approach, using uniformly smeared longitudinal reinforcement gives erroneous predictions for members reinforced with varying reinforcement along the side and adjacent panels. To mitigate the problem, for rectangular RC members, it is preferable to use the local rebar ratio assignment. To avoid double-counting of edge reinforcements, since the corner bars are shared by two adjacent panels, half the bar area will be used in the reinforcement ratio evaluation (see Fig. 18b). This method of adjusting the average reinforcement ratios with the slight modification can reasonably account for the effect of local reinforcement distribution conditions especially for lightly

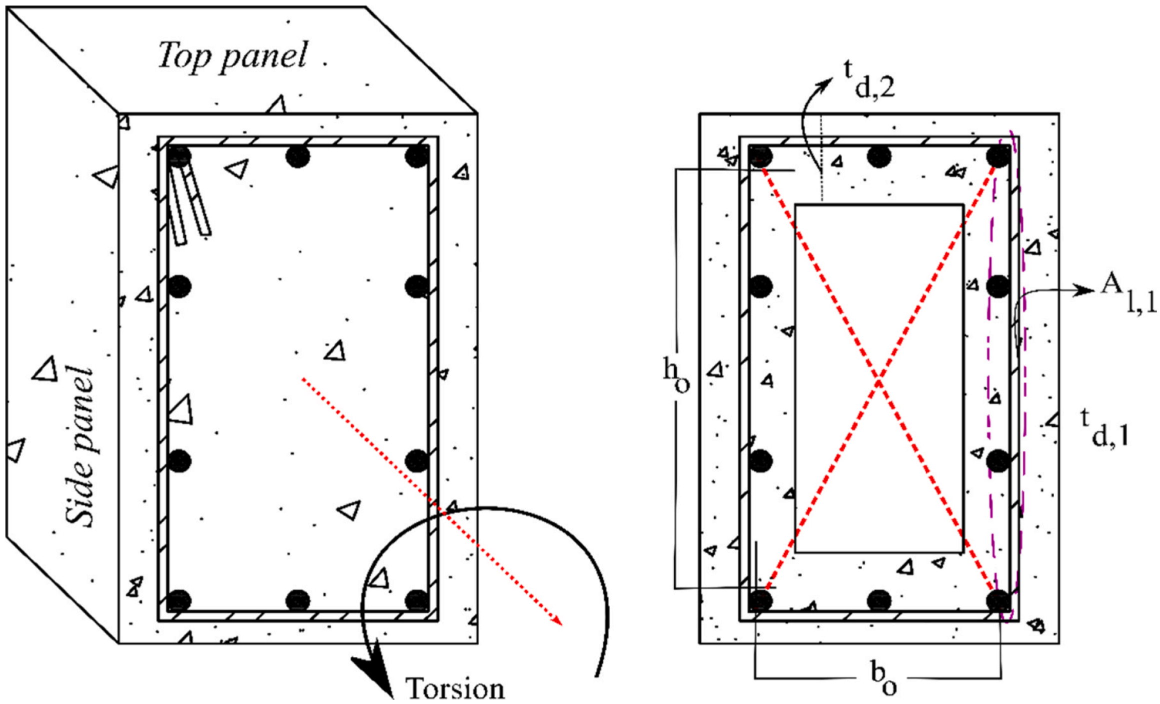

Fig. 18. (a) Top and side panel (b) Shear flow zone and local longitudinal reinforcement.

reinforcement members with a larger aspect ratio. Accordingly, the equations for longitudinal and transverse rebar ratios for each panel are given by Eqs. 5 and 6. It should also be noted that the above equation (Eq. 5) converges to the average rebar ratio for members that are symmetrically reinforced whereas it gives varying rebar rations for panels that are unsymmetrically reinforced.

$$\rho_{l,i} = \begin{Bmatrix} \dfrac{A_{l,i}}{b_o t_{d,i}} & \textit{for panel } 2 \\ \dfrac{A_{l,i}}{h_o t_{d,i}} & \textit{for panel } 1 \end{Bmatrix} \tag{5}$$

$$\rho_{t,i} = \frac{A_t}{S t_{d,i}} \quad \textit{for panel } 1 \textit{ and } 2 \tag{6}$$

The general framework of the modeling approach is presented in Fig. 19. The presented modeling approach can be easily extended to model unsymmetrical longitudinal reinforcements along the top and bottom panel by considering all four panels. The current simplified modeling with two panels (side and top) will hereafter be referred to as 2P_SMMT. Later in the section, when the modeling approach is integrated with the proposed spalling model, it is referred to as 2P_Spalled_SMMT.

The cover spalled model is incorporated into 2P_SMMT to demonstrate its capability. The solution algorism for 2P_SMMT is presented in Fig. 20. The analysis of RC members subjected to torsional action will be done following two stages. Using 2P_SMMT, a sectional analysis will be conducted incrementally, and spalling moment and spalling resistance are checked. When the limit of spalling is exceeded, the section will begin the gradual spalling process. Starting from this stage, one approach to analyzing the member is to assume the section is fully spalled and conduct the remaining analysis with the spalled dimensions. However, as presented earlier, the main deficiency of this approach is the spalling process is gradual. Thus, conducting the analysis using a sudden created fully spalled section will result in a large discontinuity (see Fig. 21).

An alternative approach and the preferred method in the current study is to use a two-stage/phase analysis. After reaching the spalling limit, the member is reasonably assumed to go through gradual spalling, and ultimately, the section will fully spall. Hence, the behavior of the gradual spalling is going to be bounded between fully intact and fully spalled analysis.

After the limit of spalling is exceeded, a sectional analysis should be done using a fully spalled section. By using the original segment up to the initiation stage of the spalling of the first analysis and the upper limit of the second analysis (see Fig. 21), the torsional envelope can be plotted. It should be noted that in the current modeling, gradual delamination of cover is not directly incorporated and reasonably assumed its behavior to be between the fully intact and the fully spalled analysis. In the current state of knowledge on the spalling of concrete cover, it is not possible to rationally incorporate a gradual spalling on sectional analysis. Thus, further investigation directed on the gradual spalling will be needed to adequately model the range between the initiation and the full spalling of the cover. The two-phase analysis method incorporating 2P_SMMT is presented in a compact solution algorism (see Fig. 22). For RC members with a small cover, the acting spalling moment will be less than the spalling resistance. Consequently, the proposed method will converge to 2P_SMMT. Whereas for members with large cover, the pre-spalling analysis will be identical to the base model. After initiation of the spalling (which is determined by the current spalled theory), the behavior of the member will be assessed using a fully spalled sectional analysis.

The capability of the Two-phase modeling is presented by comparing the prediction of the approach with the recently conducted thick concrete cover tests. Furthermore, the model (2P_Spalled_SMMT) is also checked against two additional specimens of Nagataki et al. [14].

The comparison between the proposed approach and experiment by Nagataki et al. [14] and the current set of experiments is presented in Fig. 23 and Fig. 24. For the specimens with relatively small cover, similar to the experiment, the model correctly predicted the spalling of cover occurring after the cracking torsion. Furthermore, the prediction showed the section failed due to the crushing of the strut coupled with cover spalling.

The remaining specimens were cast with a relatively thick concrete cover. The experimental results indicated the specimens prematurely failed due to the spalling of concrete cover which initiated near the

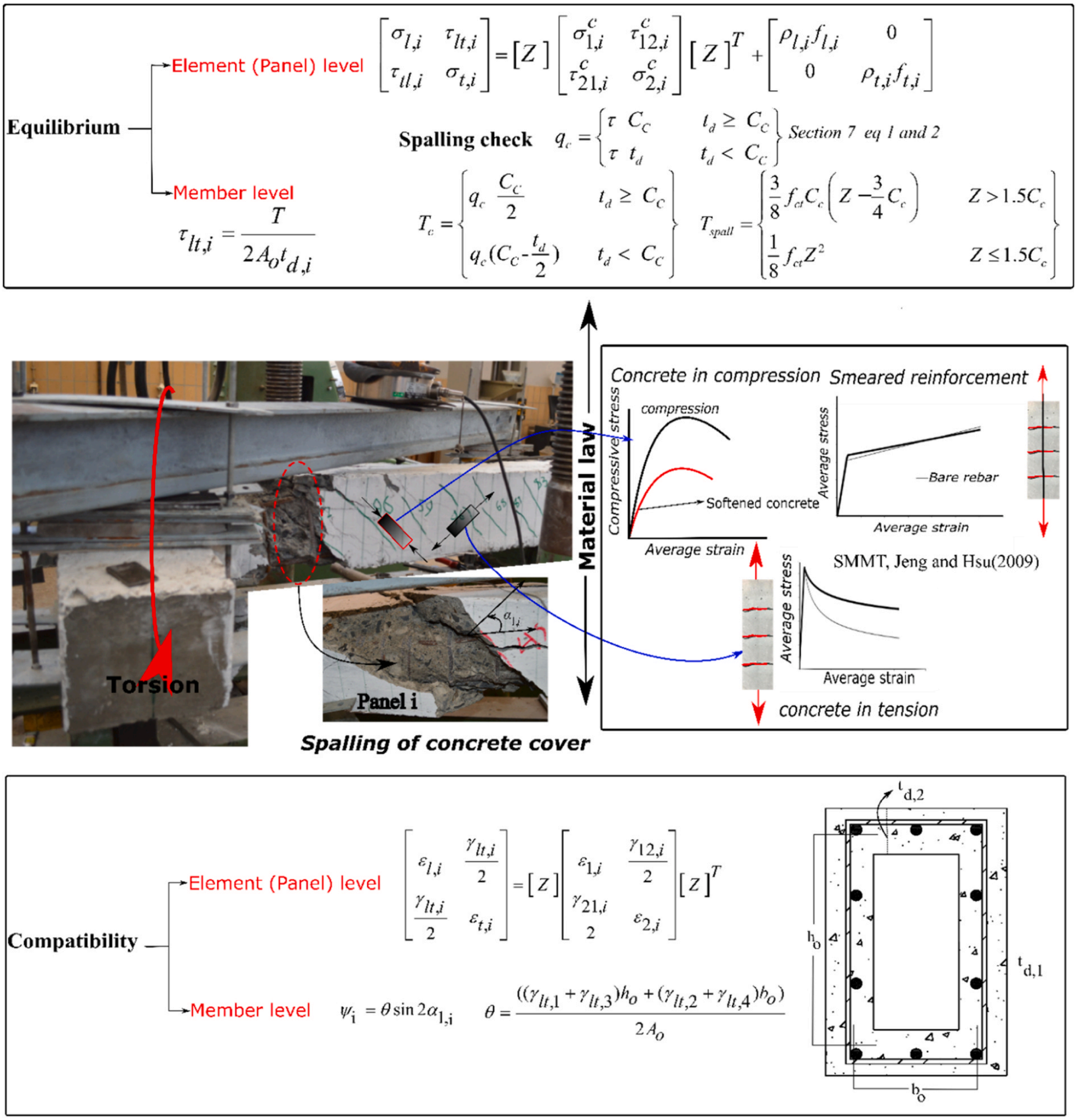

Fig. 19. General Framework of 2P_Spalled_SMMT.

cracking torsion. The proposed approach rightly predicted the members' brittle failure mode due to spalling and the initiation stage. The post-spalling prediction of the model is also consistent with observed brittle post-crack behavior. Similar to the recently tested specimen, the proposed model adequately predicted the pre and post-spalling behavior of Nagataki et al. [14] specimens. Considering the complex failure mode due to the spalling of cover coupled with the very scattered nature of the tensile strength of concrete, the prediction of the proposed approach showed a consistent prediction.

6. Comparison of the ultimate capacity prediction of the models

The proposed approach is capable of predicting the total loading history of RC members with a thick concrete cover. For members with relatively large cover, failure is associated with the spalling of cover. RC member's failure due to spalling is complex as it is dependent on numerous factors including concrete cover, the tensile strength of concrete, and rebar layout. To compare the capability of the proposed model, a comparison of the peak capacity predicted by SMMT, STM, CFT, and the proposed approach against the experiment is presented in Table 3 and Fig. 25.

Although both models give an excellent prediction for RC sections with small cover, as it can be observed from the results, SMMT and STM highly overestimated the ultimate capacity of the sections with relatively large cover concrete. Their prediction shows unsafe estimates having a large scatter. The reason for this erroneous prediction exists in the underlying modeling considerations. In both modeling approaches, a member's failure due to spalling of concrete cover is not explicitly considered. Moreover, in the models, the thickness of the concrete cover is not used as an input. Practically speaking, the models gave a false equivalence between the behavior RC members having similar cross-sectional sizes but with different concrete cover thickness.

Regarding CFT, due to the inherited conservative approach of full section spalling coupled with the model's ignorance of tensile strength

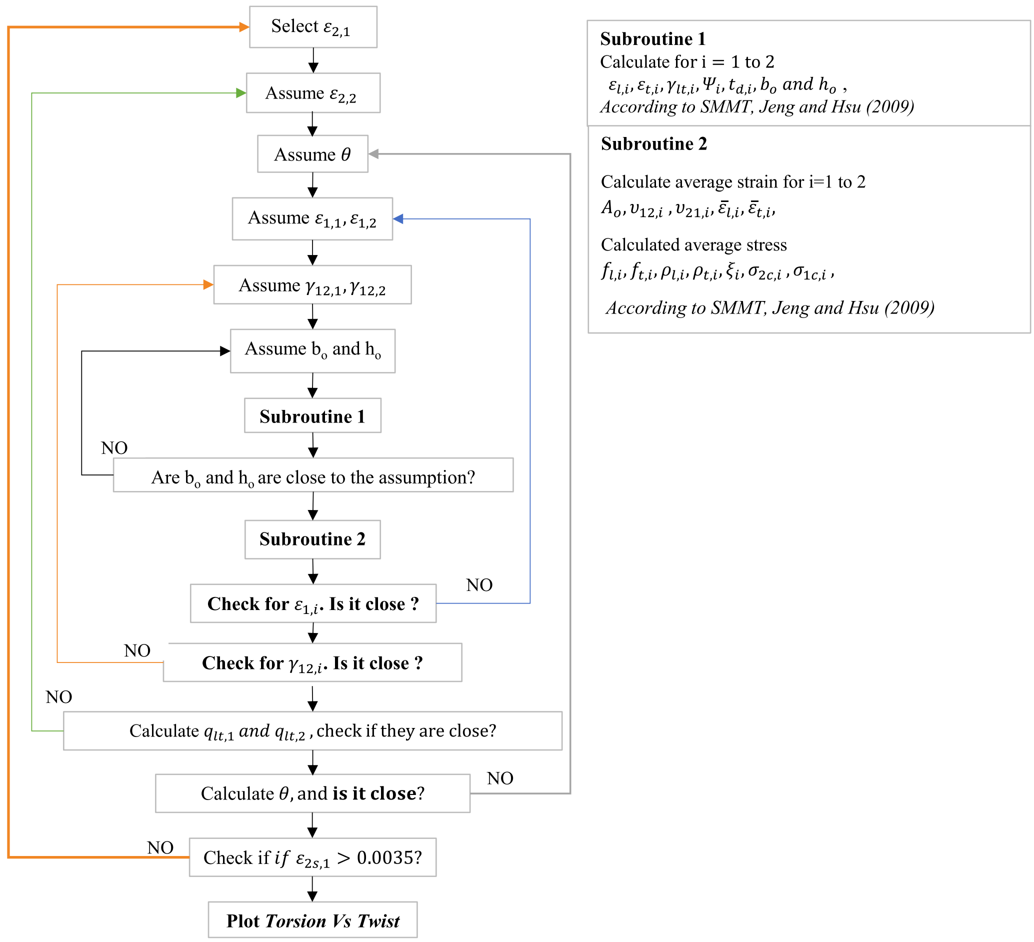

Fig. 20. Flowchart for 2P_SMMT.

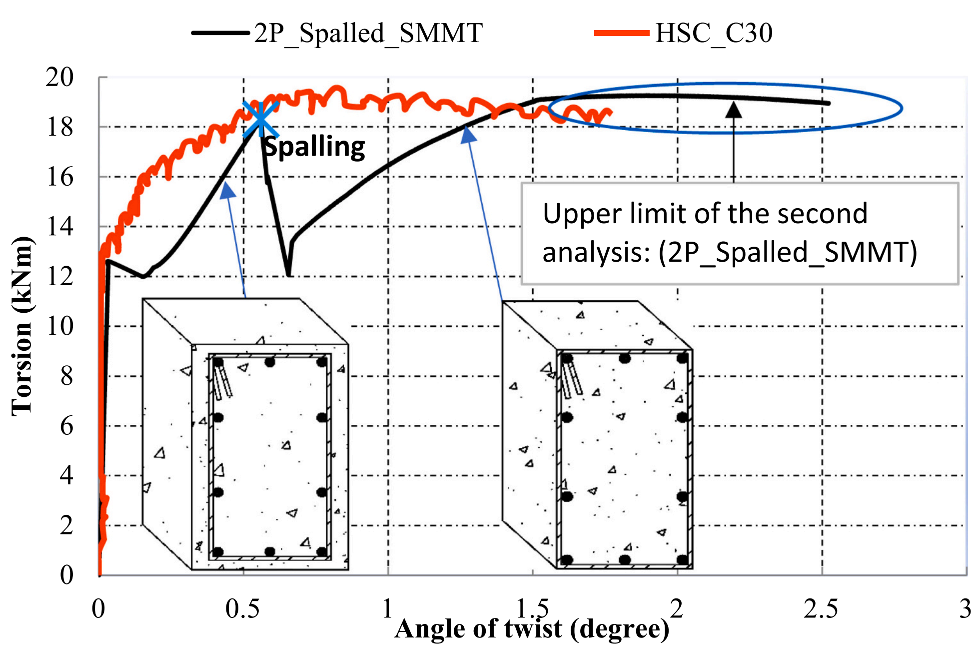

Fig. 21. Spalled analysis of specimen HSC_C30 [7].

of the concrete, the theory gave a very good ultimate strength prediction. Even though the estimate gives a closer prediction, the existing gaps in the model including the absence of compression softening of diagonally cracked concrete and assumption of spalling for small concrete cover thickness are not consistent with experimentally observed behavior.

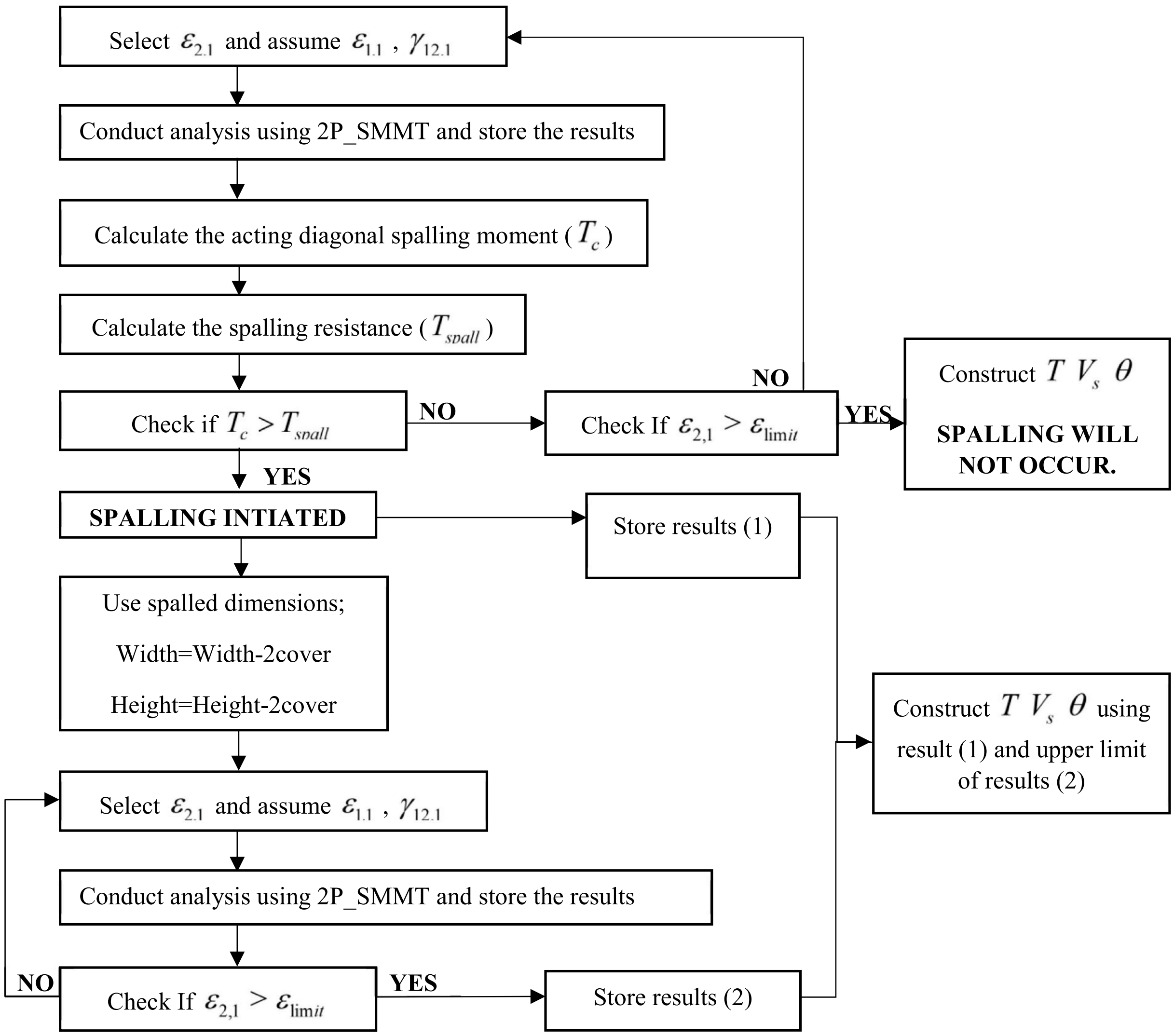

Fig. 22. Two-Phase solution algorism.

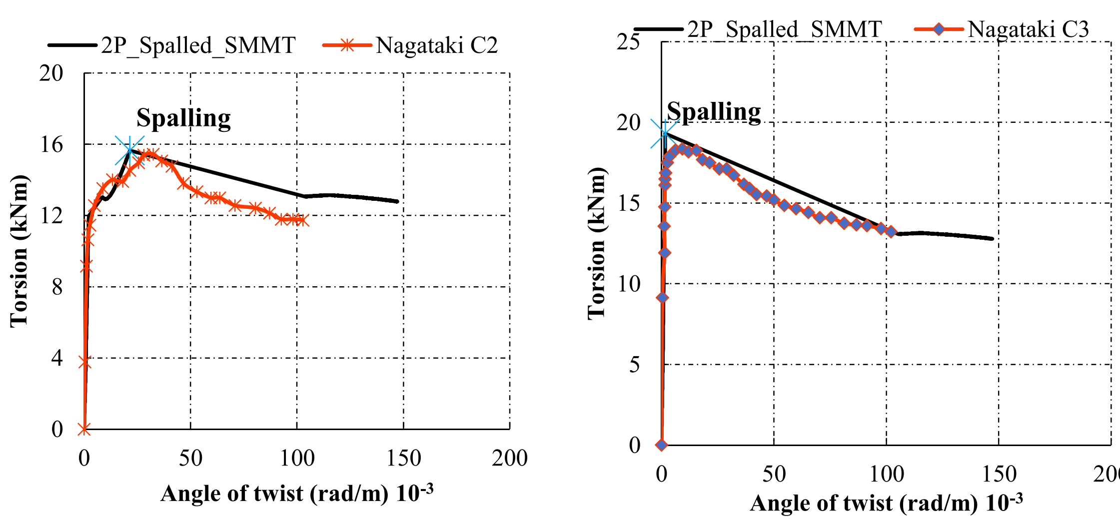

Fig. 23. Comparison between Spalled-SMMT and specimens by Nagataki et al. [14].

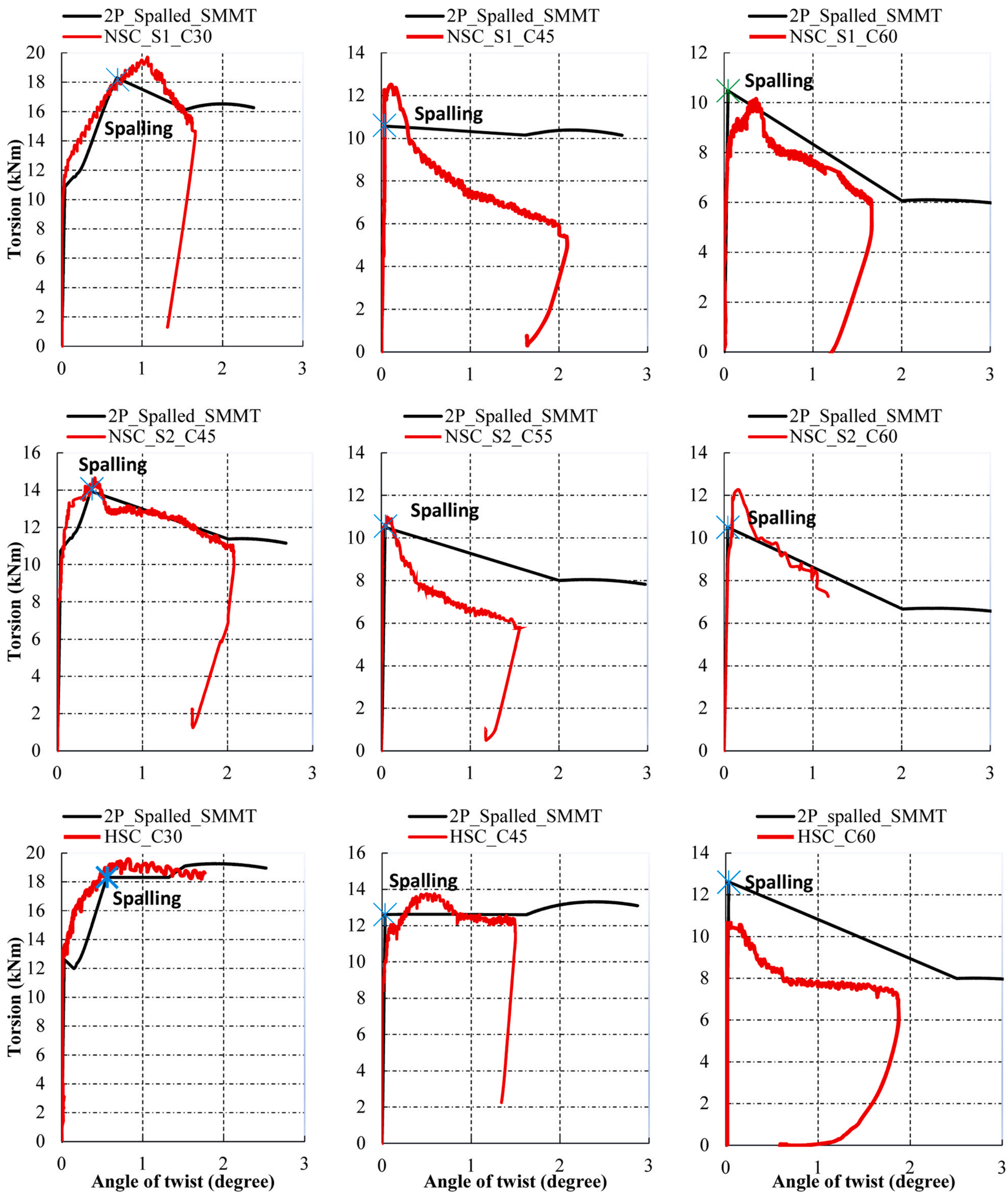

Fig. 24. Comparison between Spalled-SMMT and thick cover specimens [7].

Compared with the above models, the proposed approach which utilized the new spalling theory gave the best prediction with relatively smaller COV. The proposed method gave an average experiment to a prediction ratio of 1.04 with a COV value of less than 10 %. Although the prediction by the proposed approach gives a consistent prediction, the method should be further scrutinized using additional experiments with larger cover and varying parameters.

7. Conclusions

Research on torsional behavior of RC members has been conducted for the past 100 years and intensified in the last 50 years. These investigations improved our knowledge of the mechanics behind the torsion of RC members, and many theoretical models were developed as a result. The state-of-the-art models are verified on the domains of experimental data missing-in specimens with thick concrete cover. Nowadays, due to stringent code requirements for durability design, the use of thick concrete cover is becoming common in practice. In this

Table 3
Comparison among SMMT, STM, CFT, Spalled-SMMT with experiment.

Set	Specimen	T_{Exp} (kNm)	T_{SMMT} (kNm)	T_{STM} (kNm)	T_{CFT} (kNm)	$T_{2p\_Spalled\_SMMT}$ (kNm)	$\frac{T_{Exp}}{T_{SMMT}}$	$\frac{T_{Exp}}{T_{STM}}$	$\frac{T_{Exp}}{T_{CFT}}$	$\frac{T_{Exp}}{T_{2p\_Spalled\_SMMT}}$
1	NSC-S1-C30	19.71	23.73	19.92	22.42	18.29	0.83	0.99	0.88	1.08
	NSC-S1-C45	12.51	23.66	19.02	13.86	10.56	0.53	0.66	0.90	1.18
	NSC-S1-C60	10.15	22.46	18.87	7.89	10.47	0.45	0.54	1.29	0.97
2	NSC-S2-C45	14.66	23.34	19.49	14.79	13.95	0.63	0.75	0.99	1.05
	NSC-S2-C55	10.95	22.8	19.10	10.43	10.49	0.48	0.57	1.05	1.04
	NSC-S2-C60	12.25	22.85	19.06	8.33	10.49	0.54	0.64	1.47	1.17
3	HSC-C30	19.86	26.9	25.05	25.91	19.26	0.74	0.79	0.77	1.03
	HSC-C45	13.76	26.9	25.05	18.09	13.31	0.51	0.55	0.76	1.03
	HSC-C60	10.65	26.9	25.05	11.12	12.61	0.4	0.43	0.96	0.84
						Average	0.57	0.66	1.01	1.04
						Maximum	0.83	0.99	1.47	1.18
						Minimum	0.40	0.43	0.76	0.84
						COV	24.80	25.48	23.37	9.68

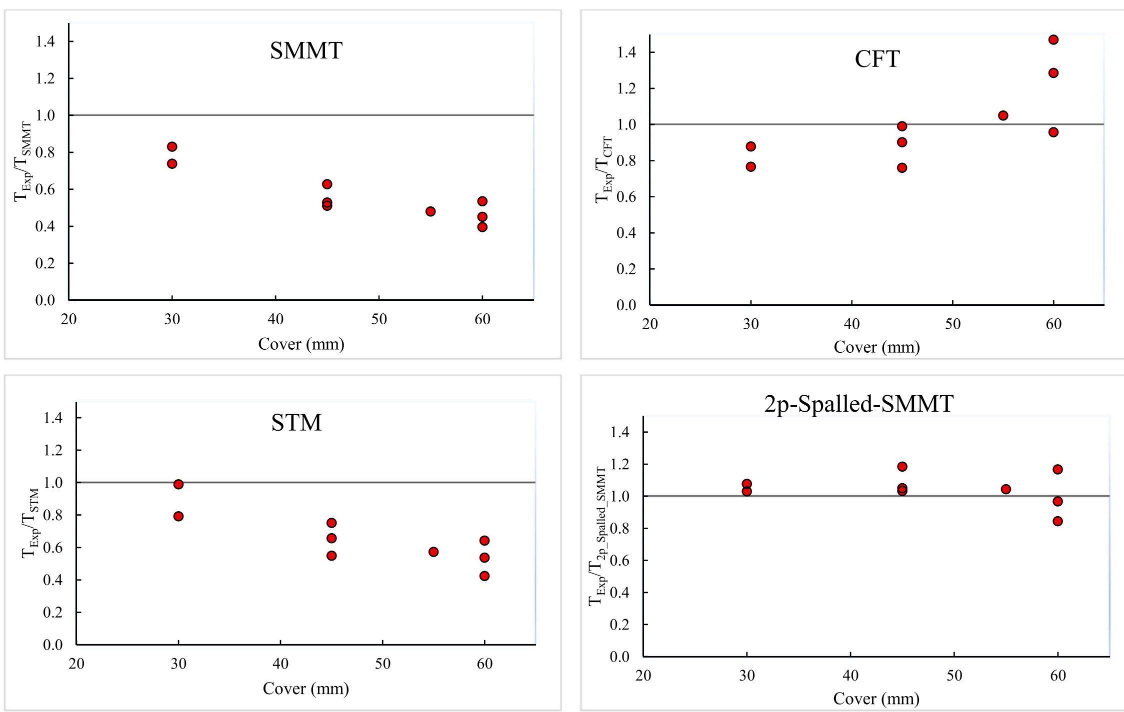

Fig. 25. Comparison among SMMT, STM, CFT, the proposed model with experiment (cover is the distance from the surface to the centroid of longitudinal rebar).

regard, the study thoroughly investigated the shortfalls in the current advanced models for concrete with thick cover and the existing spalling theories. The investigation was supported by a recently conducted torsional experimental campaign on RC members with a thick concrete cover. The following main conclusions are drawn.

1) The existing advanced models fail to predict the torsional behavior of RC members with thick concrete cover. The models either highly overestimate the ultimate capacity and give an unsafe prediction or provide erroneous overall behavior of the member. This is due to the different mechanics between RC beams with thin and thick covers.
2) The study provided a rational theory for the spalling of concrete cover due to torsion and shear. The theory is a unified approach as it can also explain cover spalling on shell elements.
3) The capability of the theory is further demonstrated by incorporating the scheme into an existing sectional analysis model (Spalled-SMMT). Using the unified rational theory and solution algorism, the proposed model is examined with the recently conducted torsional experiments and experiments from literature. The proposed approach showed consistent and reasonable modeling of RC members subjected to torsion with a large concrete cover as well.
4) While the proposed approach can predict the initiation of the spalling of concrete cover the gradual evolution of spalling is not addressed. Future developments of this study will be focused on mechanics of gradual delamination of concrete cover. Currently, a comprehensive experimental campaign is underway to investigate the complicated spalling phenomenon on RC members subjected to torsion and associated action.

CRediT authorship contribution statement

Esayas Gebreyouhannes Ftwi: Writing – review & editing, Validation, Supervision, Resources, Methodology, Formal analysis, Conceptualization. **Mohammed Sirage Ibrahim:** Writing – review & editing, Writing – original draft, Visualization, Validation, Methodology, Investigation, Formal analysis, Data curation, Conceptualization.

Declaration of Competing Interest

The authors declare that they have no known competing financial interests or personal relationships that could have appeared to influence the work reported in this paper.

Data availability

Data will be made available on request.

Acknowledgment

This research did not receive any specific grant from funding agencies in the public, commercial, or not-for-profit sectors. The Authors wish to thank Prof. Dr.-Ing Girma Z and Dr.-Ing Adil Z for the fruitful discussions. The U-shaped specimen is tested by Alyu Abdela as part of his M.Sc. thesis. The authors wish to thank for the contribution.

References

[1] Hsu TTC. Torsion of structural concrete - behaviour of reinforced concrete rectangular members (SP18-10). Acids Spec Publ 1968;18:261–306.
[2] Fang IK, Shiau JK. Torsional behavior of normal- and high-strength concrete beams. Acids Struct J 2004;101:304–13.
[3] Rasmussen LJ, Baker G. Torsion in reinforced normal and high-strength concrete beams - part 1: experimental test series. Acids Struct J 1995;92:56–62.
[4] Koutchoukali NE, Belarbi A. Torsion of high-strength reinforced concrete beams and minimum reinforcement requirement. Acids Struct J 2001;98:462–9.
[5] Mitchell D, Collins MP. Diagonal compression field theory-a rational model for structural concrete in pure torsion. Acids J Proc 1974;71:396–408.
[6] Rahal KN, Collins MP. Effect of thinckness of concrete cover on shear-torsion interaction-an experimental investigation. ACI Struct J 1995;92.
[7] Ibrahim MS, Gebreyouhannes E, Muhdin A, Gebre A. Effect of concrete cover on the pure torsional behavior of reinforced concrete beams. Eng Struct 2020;216: 110790. https://doi.org/10.1016/j.engstruct.2020.110790.
[8] Chiu HJ, Fang IK, Young WT, Shiau JK. Behavior of reinforced concrete beams with minimum torsional reinforcement. Eng Struct 2007;29:2193–205. https://doi.org/10.1016/j.engstruct.2006.11.004.
[9] Joh C, Kwahk I, Lee J, Yang IH, Kim BS. Torsional behavior of high-strength concrete beams with minimum reinforcement ratio. Adv Civ Eng 2019;2019. https://doi.org/10.1155/2019/1432697.
[10] Kim MJ, Kim HG, Lee YJ, Kim DH, Lee JY, Kim KH. Pure torsional behavior of RC beams in relation to the amount of torsional reinforcement and cross-sectional properties. Constr Build Mater 2020;260:119801. https://doi.org/10.1016/j.conbuildmat.2020.119801.
[11] McMullen AE, Rangan BV. Pure torsion in rectangular sections - a re-examination. J Am Concr Inst 1978;75:511–9.
[12] Peng X, Wong Y. Behavior of reinforced concrete walls subjected to monotonic pure torsion — an experimental study. Eng Struct 2011;33:2495–508. https://doi.org/10.1016/j.engstruct.2011.04.022.
[13] Lee JY, Kim KH, Lee SH, Kim C, Kim MH. Maximum torsional reinforcement of reinforced concrete beams subjected to pure torsion. Acids Struct J 2018;115: 749–60.
[14] NAGATAKI S, LEE SH, OKAMOTO T. A study on mechanism of torsional resistance of reinforced concrete members. Doboku Gakkai Ronbunshu 1988;1988:179–88.
[15] Leonhardt F, Schelling G. Torsionsversuche an Stahlbetonbalken. Dtsch Aussch Für Stahlbet 1974.
[16] ACI Committee 318. Building Code Requirements for Structural Concrete (ACI 318–14) Commentary on Building Code Requirements for Structural Concrete (ACI 318R-14). Farmington Hills, Mich.: 2014.
[17] Eurocode 2:Design of concrete structures - Part 1: General rules and rules for buildings. vol. 1. 2002.
[18] Lessig NN. Determination of the load-bearing capacity of reinforced concrete elements with rectangular cross-section subjected to flexure with torsion. Bet i Zhelezobet 1959.
[19] Yudin VK. Determination of the load-carrying capacity of rectangular reinforced concrete elements subjected to combined torsion and bending. Bet i Zhelezobet 1962:265–9.
[20] Collins MP, Walsh PF, Archer FE, Hall AS. Ultimate strength of reinforced concrete beams subjected to combined torsion and bending. Spec Publ 1968;18:379–402.
[21] Hsu TTC. Torsion of structural concrete-plain cocnrete rectangular sections. Spec Publ 1968;18:203–38.
[22] Elfgren L, Karlsson I, Losberg A. Torsion-bending-shear interaction for reinforced concrete beams. J Struct Div 1974;100:1657–76.
[23] Elfgren L, Karlsson I, Losberg A. Nodal forces in the analysis of the ultimate torsional moment for rectangular beams. Mag Concr Res 1974;26:21–8.
[24] Lampert P, Thürlimann B. Torsions-Biege-Versuche an Stahlbetonbalken. Bericht/ Institut Für Baustatik ETH Zürich,; 1969. p. 6506.
[25] Collins MP, Lampert P. Redistribution of moments at cracking-the key to simpler torsion design? Spec Publ 1973;35:343–84.
[26] Collins MP, Mitchell D. Shear and torsion design of prestressed and non prestressed concrete beams. PCI J 1980;25:32–100.
[27] Hsu TTC, Mo YL. Softening of concrete in torsional members - theroy and tests. Acids J Proc 1985;82:290–303.
[28] Jeng CH, Hsu TTC. A softened membrane model for torsion in reinforced concrete members. Eng Struct 2009;31:1944–54. https://doi.org/10.1016/j.engstruct.2009.02.038.
[29] Vecchio FJ, Collins MP. The modified compression-field theory for reinforced concrete elements subjected to shear. Acids Struct J 1986;83:219–31.
[30] Rahal KN. Behaviour of Reinforced Concrete Beams Subjected to Combined Shear and Torsion (PhD thesis). University of Toronto,; 1993.
[31] ACI-ASCE Committee 445. ACI 445.1R-12 Report on Torsion in Structural Concrete. Farmington Hills, MI.: 2013.
[32] Hsu TTC, Mo YL. Softening of concrete in torsional members - theroy and tests. Acids J Proc 1985;82:290–303. https://doi.org/10.14359/10335.
[33] Maekawa K, Okamura H, Pimanmas A. Non-linear mechanics of reinforced concrete. CRC Press,; 2003.
[34] Hsu TTC, Zhu RRH. Softened membrane model for reinforced concrete elements in shear. Acids Struct J 2002;99:460–9.
[35] Leu L-J, Lee Y-S. Torsion design charts for reinforced concrete rectangular members. J Struct Eng 2000:210–8.
[36] Rahal KN. Torsional strength of reinforced concrete beams. Can J Civ Eng 2000;27: 445–53. https://doi.org/10.1139/l99-083.
[37] Jeng CH, Chiu HJ, Peng SF. Design formulas for cracking torque and twist in hollow reinforced concrete members. Acids Struct J 2013;110:457–67. https://doi.org/10.14359/51685603.
[38] CAN/CSA-A23.3-04. Design of Concrete Structures. Can Stand Assoc,; 2007.
[39] Rahal KN. Torsional strength of normal and high strength reinforced concrete beams. Eng Struct 2013;56:2206–16. https://doi.org/10.1016/j.engstruct.2013.09.005.
[40] Bruun EPG, Bentz EC. Experimental procedures for displacement-controlled pure torsion tests on reinforced concrete shells. Int Conf Adv Exp Struct Eng 2017;2017-Septe:193–215. https://doi.org/10.7414/7aese.T2.76.
[41] Rahal KN, Collins MP. Analysis of sections subjected to combined shear and torsion - a theoretical model. Acids Mater J 1995;92:459–69. https://doi.org/10.14359/995.
[42] Fisher AW, Bentz EC, Collins MP. Response of heavily reinforced high-strength concrete coupling beams. Acids Struct J 2017;114:1483–94. https://doi.org/10.14359/51689501.
[43] El Mohandes F, Vecchio F. VecTor3: A. User's Manual; B. Sample Coupled Thermal and Structural Analysis. Toronto, ON, Canada: Dep Civ Eng Univ Toronto,; 2013.